Deconstructing the dissimilatory sulfate reduction pathway:

Isotope fractionation of a mutant unable to grow on sulfate

Emma Bertran

Master's Thesis

Department of Earth and Planetary Sciences
McGill University, Montreal

Supervisor: Professor Boswell Wing

August 2013

A thesis submitted to McGill University in partial fulfillment of the requirement of the Master's degree in Earth and Planetary Sciences

Table of contents

Methods

Abstract

English

Dissimilatory sulfate reduction plays a significant role in shaping the sulfur isotope composition of sedimentary sulfides. These, in turn, record the evolution of Earth's surface redox state. The fractionation produced by this microbial metabolism is controlled by the flux of sulfur through the respiratory reaction network and the isotopic effect associated with each component reaction. Although the net isotope fractionations of this metabolism have been well studied, unraveling the isotopic influence of each component of its pathway is still a challenge. The sulfite to sulfide reduction step is a particularly complicated one. Its biochemistry is not fully understood and the associated isotope effect is inferred from fractionations associated with the entire metabolic pathway or from *in-vitro* experiments with cell-free extracts. Here, two experiments, a batch and a continuous culture experiment, were run using a mutant strain of the sulfate-reducing bacterium *Desulfovibrio vulgaris* Hildenborough. This deletion mutant is missing its QmoABC protein complex, a principal catalyst in the reduction of adenosine phosphosulfate (APS) to sulfite. As APS is an intermediate metabolite between sulfate and sulfite in the respiration pathway, this strain is incapable of using sulfate as a terminal electron acceptor. By hindering APS reduction, this mutation also eliminates sulfite disproportionation. As a consequence, analysis of the growth and biochemistry of this bacterium provides a unique insight into the sulfite reduction step. In all experiments, sulfite consumption was concomitant with sulfide and thiosulfate production. However, thiosulfate production in the continuous culture experiment was more than one order of magnitude smaller than in the batch experiment. Thiosulfate can form inorganically from the reaction of aqueous sulfite and sulfide. It appears that the design of the batch experiment rendered the establishment of a definite reaction network challenging. Although it was not excluded that thiosulfate could be produced as a biochemical intermediate of sulfite reduction, the thiosulfate pool that accumulated in both the batch and the chemostat experiments was found

to be mostly of inorganic origin. Because of this, a net fractionation factor could not be extracted from the batch experiment. The chemostat experiment appeared to be better defined isotopically, and thus a net fractionation between sulfite and sulfide of -15.88 ‰, at 10% maximum bacterial growth rate, was found. The implications of such a large extent of inorganic thiosulfate production environmental settings and laboratory experiments, both in vivo and in vitro, are discussed.

French

La réduction dissimilatoire du sulfate joue un rôle important dans le façonnage de la composition isotopique des sulfides sédimentaires. Ce signal isotopique, à son tour, représente un archive important de l'évolution de l'oxygène atmosphérique. Le fractionnement produit par ce métabolisme microbien est contrôlé par le flux de soufre à travers du réseau de réactions et l'effet isotopique associé à chaque réaction. Bien que le fractionnement isotopique général de ce métabolisme ait été bien étudié, il est important de comprendre l'influence de chaque composante du réseau. La dernière étape, la reduction du sulfite en sulfide, n'est pas encore entièrement comprite. Les réactions qui la définent ne sont pas cernées et l'effet isotopique associé est, jusqu'à date, déduit de fractionnements associés à la voie métabolique dans son ensemble. Ici, deux expériences, la première dans un système fermé, la deuxième dans un système ouvert, ont été effectuées en utilisant une souche mutante de *Desulfovibrio vulgaris* Hildenborough. Cette bactérie ne possède pas son complexe QmoABC, un catalyseur principal de la réduction du phosphosulfate d'adénosine (APS) au sulfite. Par conséquent, cette souche est incapable d'utiliser le sulfate en tant qu'accepteur d'électrons. En entravant la reduction de l'APS, cette mutation élimine également la dismutation du sulfite. En conséquence, l'analyse de la croissance et de la biochimie de cette bactérie fourni un aperçu unique sur cette étape. Dans les deux expériences, la consommation du sulfite et la production du sulfide et du thiosulfate eurent lieu simultanément. Cependant, l'occurrence simultanée de réactions biologiques et non-biologiques, ces dernières formant de vastes quantités de thiosulfate à partir du sulfite et du sulfide,

a rendu la mise en place d'un réseau de réaction précis difficile. Bien qu'il n'est pas exclu que le thiosulfate pourrait être produit en tant qu'intermédiaire de la réduction du sulfite, le thiosulfate accumulé dans les deux expériences a été jugé d'origine essentiellement non-biologique. Pour cette raison, un facteur de fractionnement n'a pas pu être calculé. L'expérience de culture continue est mieux définie isotopiquement et donc un fractionnement net entre le sulfite et le sulfide de -15.88 par millions, à 10% la croissance maximale des bactéries, a été estimé. Les consequences de la production non-biologique de thiosulfate dans des environments naturels et durant des expériences de laboratoire, in vivo et in vitro, sont discutées.

Acknowledgements

E. Bertran would like to acknowledge Professor B. Wing for sponsoring and supervising this thesis work. G. Zane is immensely thanked for sharing the mutant bacterium studied here, and J. Wall's laboratory for making the production of said mutant possible. D. Johnston is thanked for his generosity in sharing lab space, equipment and insight in the interpretation of the reported results. C. Hansel is thanked for allowing use of equipement. E. Bertran would like to thank W. D. Leavitt for his teachings of laboratory techniques as well as for his input while interpreting the obtained results. A. Pellerin is thanked for his help performing the first sulfur isotope measurements of the data set. McGill University and the department of Earth and Planetary Sciences are thanked for sponsoring her Master's work, which made this thesis possible, and for all the great memories created during her stay.

Contributions

This thesis was entirely written by E. Bertran and edited by B. Wing. The mutant bacterium was produced and initially grown by G. Zane. The batch experiment and associated assays were run by E. Bertran. The chemostat experiment was performed by E. Bertran with the assistance of W. D. Leavitt, who originally taught her the assays and purification of sulfur species for isotopic analysis. Anion chromatography was run by E. Bertran with the assistance of A. Vasquez-Rodriguez in Dr. Hansel's lab. Isotopic analyses were run at McGill University (Wing lab) and Harvard University (Johnston lab) with the assistance of A. Pellerin and W. D. Leavitt respectively.

Introduction

The sulfur isotope record is a powerful tool to reconstruct the evolution of Earth's surface environmental conditions in the past (Berner and Canfield, 1989; Canfield et al, 2000; Canfield, 2001 and 2004). For instance, Farquhar et al (2000) used isotopic signatures from sulfides and sulfates in Precambrian rocks to pinpoint a major change in the sulfur cycle between 2090 and 2450 million years ago (Ma). Prior to 2090 Ma, the sulfur isotopic signal was consistent with mass-independent fractionations (which differ significantly from those expected from the relative mass ratios of the sulfur isotopes), after 2090 Ma, the signal corresponded to mass-fractination (which is given roughly by the relative mass ratios of the sulfur isotopes). This difference was proposed to reflect significant changes in Earth's atmospheric oxygen abundances such that the Archean and earliest Paleoproterozoic sulfur cycle would have been driven predominantly by photochemical reactions. Later, increasing atmospheric oxygen abundances promoted oxidative weathering, which homogenized the mass-independently fractionated sulfur reservoirs and eliminated the peculiar photochemistry, giving rise to a mass-dependent isotopic signal. Further evidence from photochemical

experiments (Farquhar et al, 2001) and atmospheric models (Pavlov and Kasting, 2002) supported this interpretation.

Although a number of processes are involved in the sulfur cycle (continental weathering, volcanic outgassing, pyrite burial, evaporite deposition; Canfield, 2004), much of it is driven by biogeochemical processes, of which sulfate-reducing bacteria (SRB) are the central actors. Via their metabolism of dissimilatory sulfate reduction (DSR), these microbes reduce environmental aqueous sulfate to aqueous sulfide, therefore promoting the formation and burial of sedimentary pyrite (FeS_2) (Garrels and Lerman, 1981; Berner, 1982; Walker, 1986; Canfield, 2004; Johnston et al, 2009). This, in turn, has a direct effect on atmospheric oxygen abundances, since about 2 moles of oxygen escape consumption through oxidation weathering for every mole of pyrite buried in deep anoxic sediments (Berner and Canfield, 1989).

Sulfide produced via DSR is depleted in ^{34}S relative to the starting sulfate. Because of its dependence upon environmental factors, such as temperature, sulfate and carbon source availability (Sim et al, 2011; Canfield et al, 2006; Habicht et al, 2006), this mass-dependent sulfur isotope fractionation has been used to infer the environmental conditions in which the SRB's dwell in the past (Strauss, 1993; Strauss, 1997; Strauss, 1999; Canfield, 2001). Additionally, the specificity of this "biosignature" allowed the origin of the DSR metabolism to be dated to >3.47 billion years ago (Ga) (Shen and Buick, 2004). Laboratory experiments with SRB's have typically yielded maximum sulfur isotope fractionation factors of around -47 ‰ (Kaplan and Rittenberg, 1964; Thode, 1991; Bolliger et al, 2001), which indicates that the ^{34}S-^{32}S ratio in the product sulfide is about 47 parts per thousand smaller than the ^{34}S-^{32}S ratio in the reactant sulfate, when normalized to the ^{34}S-^{32}S ratio in the reactant sulfate. There is, however, a striking discrepancy between these values and the range of fractionations found in natural environments, where sulfides are depleted in ^{34}S by -45 to -70 ‰ relative to seawater sulfate (Ohmoto et al, 1990).

When large fractionations between sulfate and sulfide have been observed at the anoxic-oxic interface (such as the Black Sea, Neretin et al, 2003), they have been explained via oxidative sulfur cycling inducing the large offset rather than via bacterial sulfate reduction alone (Canfield, 2001; Sorensen and Canfield, 2004). In

some hypersulfidic environments, such as the porewaters in the Cariaco Basin (Werne et al, 2003), the strong depletion observed in sulfides (-60 to -72 ‰ and -55 to -65 ‰ respectively) was explained similarly through the oxidation of sulfide produced by DSR to elemental sulfur or thiosulfate, which was later disproportionated to sulfide and sulfate (Canfield and Thamdrup, 1994; Jorgensen, 1990). However, sulfur and thiosulfate disproportionation are both inhibited by high sulfide concentrations, and it is unclear whether hypersulfidic environments have high enough levels of oxidative species to oxidize sulfide in the first place (Brunner and Bernasconi, 2005).

Because of these issues, large fractionations have started to be interpreted as arising purely from DSR. In pore waters from deep ocean sediments, strongly ^{34}S enriched aqueous sulfates have been observed (Rudnicki et al, 2001). This offset was attributed the isotope effect of bacterial sulfate reduction only, with a model derived fractionation of -77 ‰. Similar results were obtained from the interstitial waters in the Great Australian Bight (Wortmann et al, 2001). Claypool (2004) analyzed sulfur isotope fractionations from a global database of porewater sediments from the Deep Sea Drilling and the Ocean Drilling Programs with a diffusion-advection model and determined that the average sulfur isotope fractionations in marine sediments of -75 ‰.

In short, in some natural settings, disproportionation and oxidative sulfur cycling might not fully explain the sulfur isotopic signals observed, leaving only bacterial sulfate reduction as a possible process. This, in turn, implies that the upper fractionation of -47 per mil observed in laboratory settings might be in the lower limit of possibilities.

Rees (1973) built a conceptual model to describe the fractionation occurring during DSR. In this classic model the net fractionation of sulfur isotopes results from the additive isotopic effects associated with each reaction of the biochemical pathway. Three of the four steps in the reaction network are well understood, however, the sulfite to sulfide reduction step, thought to bear the strongest isotopic effect, is not fully characterized. Rees (1973) derived the isotopic effect associated with this reaction mathematically, and his value of -25 ‰ spread throughout the

literature (Farquhar et al, 2003; Brunner and Bernasconi, 2005). There is, however, no direct experimental measurement of the sulfite to sulfide fractionation factor. If this step produces a stronger than estimated isotope effect, then the higher fractionations observed in natural environments could be, at least partly, explained. It is therefore crucial to produce a reliable estimate of this fractionation factor, and to fully understand the nature of the reaction and the factors influencing it.

In addition, the Rees model assumed a unidirectional, single step character of sulfite reduction (Rees, 1973). However, the full biochemistry of this metabolic step is not yet agreed upon. Evidence from growth experiments has shown that it could occur as either a direct single step reduction (Chambers and Trudinger, 1975) or via a multi-step reaction, known as the trithionate pathway, involving the production of polythionate intermediates (mainly, trithionate and thiosulfate) that are ultimately reduced to sulfide (Kobayashi et al, 1972; Kobayashi et al, 1974; Fitz and Cypionka, 1990; Sass et al, 1992). Understanding the reaction network of this step is vital because of the additive nature of the isotopic effects contributing to the net metabolic fractionation factor. Modeling studies have attempted to predict the upper fractionation limit of the metabolism when the trithionate pathway is incorporated into the overall metabolism (Brunner and Bernasconi, 2005; Farquhar et al, 2007; Johnston et al, 2007). They have shown that such an expansion of the sulfate reduction reaction pathway produced fractionations as large as the ones observed in natural environments. It must be born in mind that the trithionate pathway might not be ubiquitous to all sulfate reducers.

Addressing this issue thus requires for the sulfite reduction step to be fully isolated from the rest of the metabolic network, and the isotopic offset between sulfite and sulfide measured. It is not enough to just grow a sulfate reducing bacterium in the presence of sulfite because: (1) the andenosine phosphosulfate (APS) to sulfite reaction is reversible, and (2) sulfite can be disproportionated to sulfide and APS (Frederikson and Finster, 2003). In the first scenario, the isotopic signal measured would correspond to the additive effects of the sulfite to sulfide step and the sulfite to APS back reaction. In the second scenario, the fractionation measured would result from the disproportionation of sulfite only. In either

situation, the biochemistry of the sulfite to sulfide step as it occurs in SRB would not be resolved. Experiments on isolated enzymes known to catalyze this step would allow the determination of the enzyme-specific fractionation factor. However, this approach is technically challenging, and would still present the problem of scaling up enzymatic processes to cellular ones.

Therefore, addressing this issue has been, to date, extremely difficult. However, it is now possible to approach it thanks to the availability of a mutant strain of *Desulfovibrio vulgaris* Hildenborough. This microbe is incapable of reducing APS to sulfite, as it is missing the protein complex promoting this reaction (Zane et al, 2010). Thus, sulfite reduction is completely isolated from the rest of the metabolism, preventing back reactions to APS and sulfite disproportionation (Pereira et al, 2011; Johnston et al, 2005). Analysis of the growth characteristics, specific biochemistry and fractionation of sulfur isotopes by this bacterium provides with a unique opportunity to understand the mechanisms behind this reaction and allows producing, for the first time, an experimental value for the isotopic effect associated with this step of bacterial sulfate reduction.

This thesis will present findings from a set of two experiments: a batch and a continuous culture experiment. The batch experiment is closed to mass transport, analogous to sedimentary porewaters with very limited exchange with the overlying water column. The continuous culture experiment, on the other hand, is open to mass transport, with fresh media constantly sweeping cells and spent media out of the system. These conditions are somewhat analogous to environments such as oceans, lakes and sediments actively exchanging with the water column. This experimental design also allows easy exploration of the relationship between the extent of fractionation of sulfur isotopes and the growth rate of the bacteria (Chambers et al, 1975; Sim et al, 2011; Leavitt et al, 2013). Additionally, the results of an abiotic experiment testing the formation of thiosulfate will be presented. Sulfite has been shown to react with sulfide in aqueous solution (Heunisch, 1977), hence, this experiment informs the contribution of abiotic reactions to the sulfite, sulfide and thiosulfate pools.

First, a detailed review of the biochemical pathways involved in dissimilatory sulfate reduction will be provided, followed by a review of the isotope modeling approaches most commonly used in the literature. Then, the specifics of the experimental designs and the protocols of the various assays used will be given. Finally, the results obtained during the two biotic experiments and the abiotic experiment are reported and compared. This information is used to constrain the biochemical network of this reaction and to determine the net fractionation factor produced by sulfite reduction. The implications for the upper limit of fractionation during microbial sulfate reduction and the impact on the sulfur isotopic signal found in environmental sulfides will be discussed.

The sulfate reduction metabolism

Sulfate reducing bacteria (SRB) actively reduce environmental sulfate to sulfide via their respiratory metabolism known as dissimilatory sulfate reduction (Peck, 1960). The biochemistry of this pathway has been extensively studied through culture experiments run under different physical and chemical conditions (Peck, 1959 and 1961; Rees, 1973; Castro et al, 2000; Detmers et al, 2001; Canfield, 2001). The reaction chain consists of four main steps: (1) sulfate uptake; (2) sulfate activation to APS ; (3) APS reduction to sulfite; and (4) sulfite reduction to the final product, sulfide.

Sulfate uptake

Extracellular sulfate is first actively imported by the cell via membrane bound sulfate transporter proteins (Pereira et al, 2011). This process also imports H^+ to maintain charge balance hence creating a proton gradient across the cytoplasmic membrane.

Sulfate activation

Sulfate activation proceeds by combining intracellular sulfate with adenosine triphosphate (ATP) in a reaction catalyzed by the enzyme ATP sulfurylase (Sat), therefore producing adenosine-5'-phosphosulfate (APS) and pyrophosphate (Robbins and Lipmann, 1958a).

Although this reaction has an unfavourable equilibrium constant of 10^{-8} (Robbins and Lipmann, 1958b; Akagi and Campbell, 1962), the hydrolysis of pyrophosphate by soluble inorganic pyrophosphatase allows for the reaction to be pulled towards the production of APS (Akagi and Campbell, 1963).

APS reduction

The reduction of APS to adenosine monophosphate (AMP) and sulfite is catalyzed by the enzyme APS reductase (Peck, 1961). During this reaction, APS transfers its sulfite group to a reduced flavin adenine moiety of the enzyme APS reductase (Peck, 1961; Ishimoto and Fujimoto, 1961). The latter becomes a sulfite adduct that then dissociates into sulfite and oxidized APS reductase (Peck et al, 1982). Over the course of this reaction, AMP is produced and recycled back into the ATP pool. Although this reaction is well understood, the mechanism by which electrons are transferred to APS reductase is still debated (Pereira, 2008).

A number of studies suggested processes for transferring electrons to APS reductase while conserving energy. Odom and Peck (1981) proposed a hydrogen cycling mechanism: electrons produced from lactate oxidation are transferred to a cytoplasmic hydrogenase, thereby producing H_2, which then diffuses to the periplasm and is reoxidized. This generates electrons that are transported across the membrane and are used in the cytoplasmic reduction of sulfate. This mechanism leaves protons in the periplasm, effectively maintaining a proton gradient. Hydrogen cycling is however unlikely to be the main energy conservation mechanism in sulfate reducers because hydrogen formation from the oxidation of lactate is

energetically unfavourable and genome analyses show that cytoplasmic hydrogenases are absent in several sulfate reducing organisms (Pereira et al, 2008).

On the other hand, Voordouw (2002) and Heidelberg et al (2004) suggested that the cycling of other reduced intermediates like carbon monoxide might contribute to energy conservation in sulfate reducing microorganisms. Nevertheless, further genome analysis showed that this mechanism is also not shared by all species of sulfate reducers (Pereira et al, 2007; Pereira et al, 2008). Wood (1978) and Lupton et al (1984) proposed a membrane bound transport chain transferring protons to the periplasm. This mechanism is further supported by the fact that electron-transport-driven proton translocation has been demonstrated for several *Desulfovibrio spp.* (Fitz and Cypionka, 1991). Plus, additional studies showed that transmembrane redox complexes are unique to sulfur reducing organisms (Matias et al, 2005; Pereira et al, 2007).

The membrane-bound QmoABC complex, first described by Pires et al (2003), has been suggested to be the main actor in the transfer of electrons to APS reductase. It is composed of three subunits, two are soluble (qmoA and qmoB) and one is membrane bound (qmoC). The role of this protein machinery in transferring electrons from the quinone pool to the enzyme is supported by the facts that the genes encoding for each subunit are found adjacent to the genes encoding for APS reductase (Pereira, 2008) and the hemes in qmoC are reduced by menaquinol analogs (Pires et al, 2003; Venceslau et al, 2010). It has also been shown that the QmoABC complex is required for sulfate reduction but not for sulfite reduction in *Desulfovibrio vulgaris* Hildenborough (Zane et al, 2010). Direct electron transfer has been reported by Ramos et al (2012).

Sulfite reduction

It has been suggested that sulfite reduction occurs via either a single six electron step reaction or as a multi-step mechanism producing a number of sulfur intermediates. The production of intermediates, mainly thiosulfate, trithionate and bisulfite, during sulfite reduction provides support for the multi-step mechanism

(Findley and Akagi, 1969, 1970; Lee, 1971; Kobayashi et al, 1969, 1972; Vainshtein, 1980; Fitz and Cypionka, 1990 and Sass, 1992). For example, Findley and Akagi (1969) and Kobayashi et al (1969, 1972) observed the formation of thiosulfate and trithionate when enzyme extracts of *Desulfovibrio vulgaris*, under a hydrogen atmosphere, were provided with bisulfite.

In the light of this evidence, Findley and Akagi (1970) postulated that sulfite reduction occurs via three consecutive, enzyme catalyzed reactions, each involving the transfer of two electrons:

$$3SO_3^{2-} + 2e^- = S_3O_6^{2-} + 2e^- = S_2O_3^{2-} + SO_3^{2-}(\text{recycled}) + 2e^- = S^{2-} + SO_3^{2-}(\text{recycled})$$

Modern structural studies suggest that the enzymes DsrAB and DsrC catalyze the reduction of sulfite to trithionate (Oliveira et al, 2008; Parey et al, 2010), which is then reduced to thiosulfate by the enzyme trithionate reductase (Drake and Akagi, 1977; Peck et al, 1982). Thiosulfate is then reduced to sulfide by thiosulfate reductase (Haschke and Campbell, 1971; Aketagawa et al, 1985; Hatchikian, 1975). All the enzymes involved in this pathway however have been only partially characterized in only a number of sulfate reducers (Ishimoto et al, 1955; Haschke and Campbell, 1971; Hatchikian, 1975; Drake and Akagi, 1977; Akagi et al, 1995).

On the other hand, studies have provided evidence against the presence of a trithionate pathway. Chambers and Trudinger (1975) examined the fate of ^{35}S during the metabolism of [^{35}S]sulfate, [^{35}S]thiosulfate, and [^{35}S]sulfate plus unlabeled thiosulfate by washed cells of *Desulfovibrio spp.,* and of [^{35}S]thiosulfate by growing cells of *D. desulfuricans.* They observed that the sulfane (the innermost sulfur) and sulfonate (the outermost sulfur) groups of thiosulfate were being reduced to sulfide by both washed and growing cells at the same rate (see figure 19 for the molecular structure of sulfite and thiosulfate). If thiosulfate was an intermediate of sulfate reduction, the sulfane group would be the immediate precursor of sulfide production and thus this atom would be reduced at greater

rates than the sulfonate group. The authors thus concluded that thiosulfate was not an intermediate of sulfite reduction, but only a metabolic by-product. They also noted that intact cells catalyzed the incorporation of ^{35}S into extracellular thiosulfate in the presence of labeled sulfate, which implies an active exchange between intracellular and extracellular thiosulfate. These observations were interpreted as evidence against the presence of a trithionate pathway during sulfate reduction.

Some have pointed out that the presence of intermediates, or even genetic material encoding for the enzymes involved in the trithionate pathway, does not mean they play a significant role during sulfate reduction. Peck and Legall (1982) argued against a functional trithionate pathway because the required enzymes are not universal to all sulfate reducers, and it is not coupled with energy conservation. They suggested that the only advantage to the production and reduction of trithionate and thiosulfate was the recycling of sulfite. In addition, Broco et al (2005) investigated the role of flavoredoxin, postulated to be involved in the thiosulfate reduction step, via genetic deletion. They found that the absence of this protein severely impaired thiosulfate reduction and limited bacterial growth on sulfite. However, growth in the presence of sulfate was not inhibited. What's more, flavoredoxin is not conserved across sulfate reducing organisms (Pereira et al, 2011). This suggests that while thiosulfate might be produced as an intermediate, it is not required for the overall metabolism of sulfate reduction.

Sulfur Isotopes

Theory and annotations

Sulfur is the tenth most abundant element on earth and has four main stable isotopes: ^{32}S, ^{34}S, ^{33}S, and ^{36}S, which contribute to 95.02, 4.22, 0.760 and 0.0136 %, respectively, of the total sulfur on Earth.

The isotopic composition of a given sulfur phase is expressed using the per mil (‰) difference in the phase's isotopic ratio and the Cañón Diablo Troilite Standard. For major sulfur isotopes:

$$\delta^{34}S = \left(\frac{\left[{}^{34}S/{}_{32}S \right]_{sample}}{\left[{}^{34}S/{}_{32}S \right]_{standard}} - 1 \right) x\ 1000 \qquad (1)$$

While, for minor isotopes, the corresponding heavy to light ratios ($^{36}S/^{33}S$) are used.

Relative isotopic abundances in different co-existing phases results from the fact that lighter isotopes form bonds that acquire higher vibrational energy than heavier isotopes, making them easier to break. The rate constant of reactants bearing lighter sulfur isotopes is as a consequence higher than the rate constant of those bearing heavier isotopes (Canfield, 2001). Thus, in irreversible reactions, this difference in reaction rates will yield a net kinetic fractionation, effectively enriching the product in light isotopes. Fractionations between two co-existing sulfur species (for example, reactant A and product B) can be expressed as the ratio of their heavy to light ratios (annotated as R_A and R_B for sulfur species A and B respectively). For major isotopes:

$$^{34}\alpha_{(B\text{-}A)} = (^{34}S/^{32}S)_B/(^{34}S/^{32}S)_A = R_B/R_A \qquad (2)$$

While, for minor isotopes, the corresponding heavy to light ratios ($^{33}S/^{32}S$, $^{36}S/^{32}S$) are used. This unit-less alpha value can be used to determine $^{34}\varepsilon_{(B\text{-}A)}$, with units of ‰:

$$^{34}\varepsilon_{(B\text{-}A)} = (^{34}\alpha_{(B\text{-}A)} - 1)\ x\ 1000 \qquad (3)$$

The $^{34}\varepsilon_{(B\text{-}A)}$ value is nearly equivalent to the difference in isotopic composition between two phases of interest:

$$^{34}\varepsilon_{(B\text{-}A)} = \delta^{34}S_B - \delta^{34}S_A \quad (4)$$

High precision measurements of $^{34}\alpha_{(B\text{-}A)}$ and $^{33}\alpha_{(B\text{-}A)}$ show that these values are related by exponential factors that range between 0.500 and 0.52 as a function of mass-balance, physical conditions (such as temperature) and the specific process producing the fractionation (equilibrium, kinetic, gravitational) (Hulston and Thode, 1965; Craig et al, 1988; Mook, 2000; Young et al, 2002). These relationships can be described by Δ notation:

$$\Delta^{33}S = \delta^{33}S_{observed} - \delta^{33}S_{expected} = \delta^{33}S - 1000 \times \left[\left\{1 + \frac{\delta^{34}S}{1000}\right\}^{0.515} - 1\right] \quad (5)$$

and

$$\Delta^{36}S = \delta^{36}S_{observed} - \delta^{36}S_{expected} = \delta^{36}S - 1000 \times \left[\left\{1 + \frac{\delta^{34}S}{1000}\right\}^{1.90} - 1\right] \quad (6)$$

Where the above exponents (0.515 for ^{33}S and 1.90 for ^{36}S) are reference values for single-step thermodynamic equilibrium isotope exchange effects at low temperature (Hulston and Thode, 1965; Farquhar and Wing, 2003, 2005). The Δ notation is typically used for a single phase while for a pair of phases related by mass-dependent effects (Farquhar and Wing, 2003), exponents can be directly calculated as (Miller, 2002):

$$^{33}\lambda_{observed} = \frac{\ln\left(1+\frac{\delta^{33}S_A}{1000}\right) - \ln\left(1+\frac{\delta^{33}S_B}{1000}\right)}{\ln\left(1+\frac{\delta^{34}S_A}{1000}\right) - \ln\left(1+\frac{\delta^{34}S_B}{1000}\right)} \quad (7)$$

and

$$^{36}\lambda_{observed} = \frac{\ln\left(1+\frac{\delta^{36}S_A}{1000}\right) - \ln\left(1+\frac{\delta^{36}S_B}{1000}\right)}{\ln\left(1+\frac{\delta^{34}S_A}{1000}\right) - \ln\left(1+\frac{\delta^{34}S_B}{1000}\right)} \qquad (8)$$

Open systems

In open systems, the isotopic composition of the sulfur species being transformed is linearly related to the extent of the original compound remaining, as shown in the figure below, from Canfield (2001), which describes the evolution of the isotopic composition of sulfate and sulfide during sulfate reduction in open system conditions.

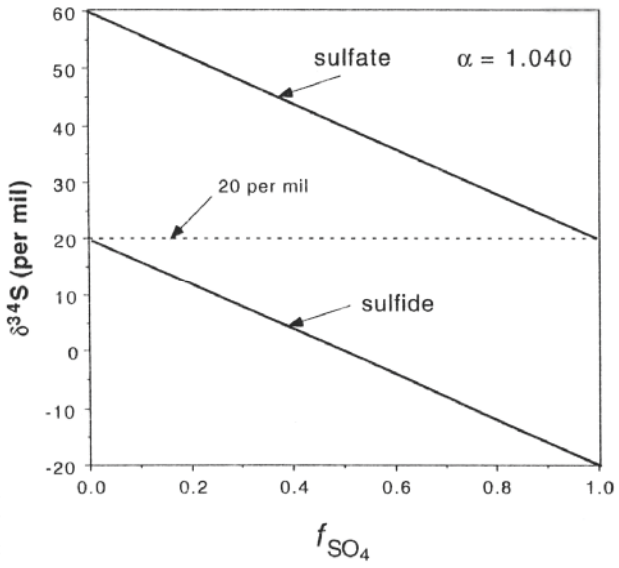

Figure 12. Indicates how the isotopic composition of sulfate and sulfide evolve in an open, well mixed, system with the same fractionation and initial isotopic composition of sulfate as in Figure 10. The parameter f_{SO_4} expresses the remaining fraction of the original sulfate in the system. See text for details.

In this system, the fractionation between the co-existing sulfate and sulfide can be expressed as:

$$\alpha_{Sulfide-Sulfate} = \frac{[\delta^{34}S_{Sulfide} + 1000]}{[\delta^{34}S_{Sulfate} + 1000]} \qquad (9)$$

The isotopic composition of the system at any given point in the extent of the reaction can be determined using the following relationships:

$$f_{SO4} + f_{H2S} = 1 \qquad (10)$$

$$\delta^{34}S_{SO4}f_{SO4} + \delta^{34}S_{H2S}f_{H2S} = \delta^{34}S_{SO40} \qquad (11)$$

Microbial metabolic models

General network model

The simplest way to understand the fractionation of sulfur isotopes during microbial sulfate reduction is through reaction networks. In these, reactants undergo a stepwise reduction, each reaction being characterized by a specific isotopic effect. If we take the following simple network consisting of three steps:

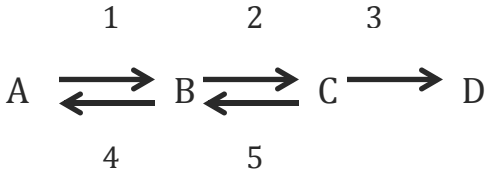

Where A, B, C and D are sulfur compounds, A is the starting species, B and C are intermediates and D the final product. Arrows 1 and 4, 2 and 5 and 3 represent the forward and backward fluxes of sulfur material between pools at steps 1, 2 and 3 respectively. Each step in the network bears a characteristic isotopic effect (in biological systems, these are kinetic and enzyme-catalyzed), which is expressed as the difference in isotopic compositions between the pools of interest. Note that, as explained earlier, fractionation occurs when bonds formed with sulfur isotopes (in the case of sulfate reduction, sulfur-oxygen bonds) are broken. Therefore, in the above reaction network, each step is assumed to involve the breaking of a sulfur

bond. Reactions in which this does not happen present no isotopic effect. The degree of flow between pools is defined as X_1 and X_2, the ratios of backward to forward flux at steps 1 and 2 respectively. Since step 3 is unidirectional, no backward flow occurs and X_3 is not defined.

The isotopic fractionation produced by the overall network equals the sum of the step specific isotopic effects weighted by the backward to forward flow ratios:

$$\delta^{34}S_{total} = \delta^{34}S_{f\_1} + X_1 . \delta^{34}S_{f\_2} + X_1 . X_2 . \delta^{34}S_{f\_3} \qquad (12)$$

Under thermodynamic equilibrium conditions, backward and forward flows become equal (and their ratios approach unity), therefore, the total isotopic effect corresponds to the sum of the isotopic effects alone. The same rationale applies to minor isotopes.

Fractionation of sulfur isotopes in microbial sulfate reduction

As explained earlier, the metabolism of microbial sulfate reduction consists of four main steps. The net fractionation produced by the overall reaction network thus corresponds to the sum of the isotopic effect of each reaction. Harrison and Thode (1958) observed a fractionation of +3 ‰ when they grew sulfate-reducers at very low sulfate concentrations (10 μM). Habicht et al (2002), observed a range -5.9 to +4.5 ‰ associated with the uptake of sulfate when growing different freshwater and marine natural populations at low sulfate concentrations. In his model, Rees assigned a +3 ‰ value to the first step of the reaction pathway, and the value spread in the literature is now widely used.

Reactions in which sulfur-oxygen bonds are not broken or that don't affect the oxidation state of sulfur have small to no isotopic effect. Therefore, the isotopic effect associated with the activation of sulfate to APS is zero. Regarding the APS to sulfite reduction step, Rees (1973) observed that most culture experiments produced upper fractionations of -25 ‰, with few exceptions presenting stronger

fractionations of up to -47 ‰ (Harrison and Thode, 58; Kaplan and Rittenberg, 64; Kemp and Thode, 68; Chambers et al, 76; Canfield, 2001). He considered the sulfite to sulfide step to be fast and irreversible, suggesting a backward flux near zero. Because of this, Rees (1973) assumed the sulfite to sulfide isotopic effect to be only rarely expressed. Therefore, he assigned a value of -25 ‰ to the APS to sulfite reduction step. Farquhar et al (2003) calculated the theoretical equilibrium sulfur isotope fractionation between sulfate and sulfite and obtained a value of -25 ‰, hence further supporting Rees's estimate for the APS to sulfite step. The sulfite to sulfide step also contributes to the overall fractionation and a -25 ‰ value was assigned to it, thus matching the observed larger fractionations. At thermodynamic equilibrium, and using these isotopic effects, Rees estimated a net upper fractionation limit of -47 ‰.

However, Rees' estimate of the sulfite to sulfide isotopic effect heavily relies on the assumption about the unidirectionality of this reaction. In addition, there is an extensive body of literature arguing for the manifestation of a trithionate pathway. Brunner and Bernasconi (2005) proposed a revised Rees model that mathematically incorporated this pathway. For this, the authors brought three important modifications: (1) they allowed for the production of a k number of sulfur intermediates; (2) they assumed the sulfite to sulfide reaction to be fully reversible, which implies the reactions producing intermediates to be reversible as well; and (3) they added an exchange flux between intracellular and extracellular sulfide. Keeping the isotopic effect associated with the uptake and release of sulfate by the cell at +3 and 0 ‰ respectively, the authors estimated the isotopic effect associated with sulfite reduction as the difference between the equilibrium isotope fractionation between sulfite and sulfide and the characteristic isotopic effect of the backward sulfide to sulfite reaction (O'Leary, 1977; Brunner and Bernasconi, 2005). The former was determined by Farquhar et al (2003) to be -48 ‰, while the latter, the abiotic sulfide to sulfite oxidation reaction, was found to be around -5 ‰ (Fry et al, 1988). Given these two estimates, it was concluded that the sulfite to sulfide step produced an isotopic effect of -53 ‰. Taking this new estimate into account, Brunner and Bernasconi (2005) estimated an upper fractionation limit for DSR of -

70 ‰. This estimate was further supported by Johnston et al (2007), who expanded the reaction network to incorporate the production of sulfur intermediates and thus added an extra flux term between sulfite and a pool consisting of said intermediates. They predicted an upper net fractionation limit of -75 ‰. These new estimates showed the effect of larger internal fractionations on the net fractionation produced by the overall metabolism.

JW9021

The bacterium used to address these questions is a mutant strain of *Desulfovibrio vulgaris* Hildenborough. This microorganism, referred to as JW9021, was provided by Dr. Grant Zane and Prof. Judy Wall, University of Missouri (Zane et al, 2010).

JW9021 is a deletion mutant missing the gene encoding for the QmoABC complex. This membrane-bound protein complex is argued to be responsible for the transfer of electrons from the membrane menaquinone pool to the enzyme AprAB (Pires et al, 2003; Venceslau et al, 2010; Pereira et al, 2008), which promotes the reduction of APS into sulfite.

The gene encoding for this protein complex was deleted via marker exchange mutagenesis. A plasmid (small strand of circular DNA) was first introduced in the microorganism. This plasmid contained a marker gene (in this case, a kanamycin resistance cassette) whose flanking sequences were identical to the ones flanking the target gene. This sequence similarity caused a phenomenon known as homologous recombination, in which the target gene is swapped off the bacterium's DNA and is effectively replaced by the marker gene (Zane et al, 2010).

Zane et al (2010) did not observe detectable growth (measured as changes in optical density, whole-cell protein concentrations and sulfide concentrations) of JW9021 in the presence of sulfate as electron acceptor. However, when the mutant was grown in the presence of sulfite, whether the electron donor was lactate of pyruvate, its growth was comparable to that of the wild-type strain (Zane et al,

2010). In order to ensure that the observed effects resulted from the deletion of the *qmoABC* genes, the authors performed a complementation experiment. A plasmid containing the deleted genes was introduced into the bacterium. In the presence of sulfate, growth rates comparable to the wild-type's were observed. Growth with sulfite as the only electron acceptor was not affected. These results were interpreted as evidence that the QmoABC complex is the only protein machinery involved in the reduction of APS to sulfite. Since growth on sulfate was not observed even after extensive culturing (over 150 hours), no other protein complex, despite the structural similarities, was able to restore sulfate reduction (Zane et al, 2010).

Thus, this bacterium is incapable of performing the APS reduction step. It bears a modified metabolism in which sulfite reduction is completely isolated from the rest of the pathway. The consequences of this modification go further: the disproportionation of sulfite produces both sulfide and APS (Frederikson and Finster, 2003). By impeding the APS to sulfite reaction, and thus the sulfite to APS back reaction as well, this mutation prevents sulfite disproportionation from occurring alongside sulfite reduction. Therefore, this bacterium's metabolic reaction network is well-suited to address the issues associated with the sulfite reduction step in DSR.

Methods

Batch experiment

Growth medium

JW9021 was grown anaerobically at 24^{o}C in a defined (MO) medium of the following composition (Zane et al, 2010): 8mM $MgCl_2$, 20 mM NH_4Cl, 0.6 mM $CaCl_2$, 2 mM K_2HPO_4-NaH_2PO_4, 6 mL/L trace metals, 30 mM Tris-HCl (pH: 7.4), 1 mL/L Thauers vitamins (10X), 60 mM lactate, 80 mM Na_2SO_3. Resazurin was added as an oxygen indicator (150 μL of a 0.1 % solution per liter of media) while titanium

citrate was used as reducing agent (5 mL per liter; pH was set at 7.2 via titration with 5 M HCl.

Anaerobic conditions were reached by first mixing the components in a bottle and subsequently performing a gas exchange in the headspace (N_2, 5 psi). Finally, the bottle was capped and autoclaved at 121^{o}C for 30 min. Autoclaving causes re-precipitation of titanium citrate and sulfite disproportionation, therefore these two components had to be added via a 0.2 μm sterile filter post-autoclaving. Stock solutions of both of these components were kept in anaerobic conditions at all times.

Experimental design

A total of 43 bottles containing 50 mL final medium volume were prepared and inoculated at the same time (the inoculum represented 6 % v/v of the media volume). At regular time intervals, three bottles were selected at random. From each, two 1 mL sub-samples were taken for OD_{600} measurements (measured in real time) and two 1 mL sub-samples were taken for protein concentration estimates (preserved at -80^{o}C). Then, 5 mL of a 20% $ZnCl_2$ solution was added to fix all sulfides in solution and arrest growth. A set of two 1mL sub-samples were taken for the estimation of sulfite, sulfide, and thiosulfate concentrations and preserved at -80^{o}C. The remaining volume was preserved at -20^{o}C for isotopic analysis. The experiment was run for 115 hours. To account for background effects, two sets of bottles at time zero were sampled, one before and one after inoculation.

Chemostat experiment

Growth medium

The defined medium used for the chemostat experiment (CS medium) was only of slightly different composition from the MO medium described above (per liter of medium): 2.87 mM K_2HPO_4, 5.67 mM ascorbic acid, 17.86 mM $NaHCO_3$, 0.4081 mM $CaCl_2$-$2H_2O$, 7.9976 mM $MgCl_2$-$6H_2O$, 18.7 mM NH_4Cl, 1mL of a 10X vitamin solution, 10 mL of a 100X trace metal solution, 1 mL of a 100 X sodium selenite solution, 20 mM sodium sulfite, 10 mM sodium lactate and 0.2 μg kanamycin (final concentration: 200 μg/mL). The last nine components were added via sterile syringe and filter post-autoclaving the media at 121°C for 30 minutes. The pH was set to 7.2 by bubbling the media under N_2:CO_2 (90:10, 5 psi) and titration with 6N HCl.

The kanamycin final concentration was chosen to be 200 μg/mL as it proved effective at selecting JW9021 over the wild-type strain without hindering its growth (Zane et al, 2010). Stock solutions of all constituents were kept anaerobic and autoclave sterile at all times, except for the vitamins, the trace metals and the sodium sulfite solutions. These were kept anaerobic and filter sterilized.

Experimental design

The continuous culture experiment was performed using a chemostat (chemical environment in static). This design allows growing bacterial populations at a specific growth rate for an indefinite period of time by imposing the rate of delivery of a chosen limiting nutrient. Here, lactate was chosen: its concentration was lowered to 10 mM, effectively limiting growth while yielding measureable optical density levels (OD_{600}).

The device included three inter-connected vessels. All surfaces consisted of glass, polyether ether ketone (PEEK) or polytetrafluoroethylene, avoiding re-

oxidation of biogenic sulfide (either in aqueous or gaseous form). The central vessel, the reactor (six-port, 3-L working volume vessel, 1964-06660, Bellco Glass), contained bacteria growing in a continuously homogenizing medium (final volume: 0.5L). Sterile medium with limiting lactate (10 mM) and excess sulfite (20 mM) was fed into the reactor from a 10L batch. Outflowing medium was collected in a 2L bottle containing 20 mL of 1% $ZnCl_2$ solution (liquid trap, L). Input and output fluxes, set at the same rate, were imposed by pumps (Ismatec four-channel Reglo analog peristaltic pump with Tygon HC F-4040-A tubing). Produced H_2S (gas) was collected as zinc sulfide in a bottle containing 50 mL 20% (wt/vol) zinc acetate, buffered with glacial acetic acid (60 $mL.L^{-1}$) (gas trap). The reactor's pH was kept constant (7.2 +/- 0.1) thanks to a pH-meter connected to an acid pump: when the pH increased beyond the set value, the pump injected concentrated HCl into the vessel. The entire apparatus was kept under positive pressures of N_2:CO_2 gas (90:10, 5 psi), maintaining the system anaerobic and ensuring the full transfer of H_2S into the gas trap. All components of the set up were autoclave sterilized before the start of the experiment. Sterile medium for the reactor was prepared in a separate bottle (according to the protocol explained earlier) and was transferred under N_2:CO_2 (90:10, 5 psi) via syringe and sterile filter. 30 mL of a mid-exponential culture, grown in batch conditions and transferred at least 3 times to ensure adaptation to the medium, was used as inoculum. It was allowed to grow in batch conditions (only gas flux) and reach mid-log OD_{600} levels before the liquid pumps were turned on.

A 10 % maximum growth rate experiment was run. Since the maximum growth rate, in batch conditions, was found to be 3.6 per day, the specific dilution rates were set at 0.36 per day. Keeping the final volume of the reactor at 0.5L, the input flow (and thereby the output flow) becomes 0.18 L/d.

Sampling

Samples were taken from the reactor, the reserve media batch, the liquid and gas traps at regular time intervals for OD_{600} measurements (measured in real time), estimation of lactate, acetate, sulfite, sulfide and thiosulfate concentrations and isotopic analysis. All samples were preserved at -20°C.

One sampling event consisted of the following steps.

(1) The liquid trap was changed with another 2 L bottle containing 20 mL of 1% $ZnCl_2$. The final volume collected over the given time interval was recorded in order to determine outflow rates. Then, subsamples were taken for isotopic analyses (two samples of 50 mL each), lactate and acetate measurements (1.0 mL combined with 0.5 mL of a 600 mM formaldehyde solution), sulfide, sulfite and thiosulfate concentration estimations (1.5 mL each).

(2) The gas trap was changed with another bottle containing 50 mL of 20% zinc acetate solution. A 1.5 mL subsample was taken for estimation of sulfide levels, the rest (48 mL) was preserved for isotopic analysis.

(3) A 10 mL sample was taken from the reactor. 1 mL was used right away for OD_{600} measurements while the rest was combined with 1 mL of anoxic 0.1% $ZnCl_2$ (previously bubbled in N_2) to fix the sulfides. Then, subsamples were taken for the determination of lactate and acetate, sulfide, sulfite and thiosulfate concentrations (volume and treatment were the same as for the liquid trap subsamples). The remaining 6 mL were preserved for isotopic analyses. Any volume taken from the reactor was replaced with the same volume of lactate-free CS medium.

The reserve media batch was sampled every second sampling time for OD_{600}, sulfite, sulfide, thiosulfate, lactate and acetate estimates. Samples for isotopic analyses were taken at the start and the end of the experiment.

Abiotic experiment

Experimental design

The experimental design used to test the formation of thiosulfate in abiotic conditions was identical to the one used for the biotic experiment. Sulfite and sulfide were added via syringe and through a sterile 0.2 μm filter to 20 bottles containing MO media (pH and anoxic conditions identical to the biotic experiment ones). At each sampling time, two bottles were selected at random. 0.2 mL of a 20 % zinc chloride solution (previously bubbled under N_2) was then added to each bottle, thereby fixing the sulfides. 1 mL sub-samples were taken for the estimation of sulfite, sulfide and thiosulfate levels and preserved at -20°C. The leftover liquid was preserved at -20°C for isotopic analysis.

Four experiments combining different sulfite:sulfide ratios (in mM) were run: 80:0 (control experiment), 80:5, 80:10 and 80:15. Sulfite was kept in far excess relative to sulfide, whose range of concentrations (from 0 to 15 mM) was chosen to match the ranges observed in the biotic experiment.

Assays

OD_{600}

Optical densities were measured in real time at 600nm using a UV-light spectrophotometer.

Fuschin (adapted from Grant, 1947)

Samples containing sulfite were diluted on ice using anoxic milli-q water (bubbled with N_2 for at least 20 min) so that their final concentration fell in the 0 to 250 μM range of the calibration curve. Zinc sulfides and cells were removed either

via centrifugation (12,000 g at 4°C for 15 min) or via filtration through sterile 0.2 μm filters under N_2.

The standards used to build the calibration curve were prepared on ice by diluting a 100 mM $NaSO_3$ solution using anoxic milli-q water. In order to account for the presence of extra Zn^{2+} and Cl^- in the samples, $ZnCl_2$ was added to the standards, which were centrifuged/filtered in the same manner as the samples. Standards were run alongside the samples every time.

0.1 mL sample or standard was then combined with 0.7 mL anoxic water and 0.1 mL of 0.04% (w/v) Pararosaniline HCl and 10% H_2SO_4, mixed, and allowed to react for 9 min. Next, 0.1 mL of 3.7% formaldehyde was added. The solution was mixed and allowed to react for 9 min. Finally, 0.75 mL of the mixture was combined with 0.75 mL anoxic milli-q water, the solution's absorbance measured at 570 nm and compared with the standard curve.

Cline (modified from Cline, 1969; reagents used were obtained from the LaMotte Sulfide Test kit, catalogue number: 3654-01-SC)

Samples containing sulfide in the form of zinc sulfide were diluted on ice using anoxic milli-q water (bubbled with N_2 for at least 20 min) until their final concentration fell in the 0 to 250 μM range of the calibration curve.

Standards were prepared on ice by diluting a 100 mM sodium sulfide solution (prepared by adding 0.24015 g sodium sulfide nonanhydrate to a 10 mL solution of 150 mM zinc chloride under N_2) down to the 0 to 250 μM range. Standards were run alongside the samples every time the assay was run. The reagent solution used for the assay consisted of 80 μL N,N-dimethyl-p-phenylenediamine sulfate and 25 μL ferric chloride, for a final volume of 105 μL. 645 μL anoxic milli-q water was combined with 105 μL reagent solution and 250 μL of sample or standard. The mixture was then allowed to react in the dark for 20 min, and the resulting absorbance measured at 670 nm and then compared with the calibration curve.

Cyanolysis (adapted from Sorbo, 1957; Kelly et al, 1969; Kelly and Wood, 1994)

Samples containing sulfides in the form of zinc sulfide were either centrifuged (12,000 g at 4°C for 15 min) or filtered through a sterile 0.2 μm filter under N_2. Standards (ranging from 0 to 25 mM) were prepared on ice with anoxic milli-q (bubbled with N_2) by diluting a 500 mM sodium thiosulfate solution down to the 0 to 25 mM working range. Standards were run alongside the samples every time the assay was made.

The assay itself consisted of the following steps:

(1) On ice, 1.6 mL of buffer solution (500 mL 0.2M $NaH_2PO_4*H_2O$ and 330 mL 0.2M NaOH; pH set at 7.0) was combined with 0.1 mL standard or sample and 1.3 mL anoxic milli-q water. 2 mL of 0.1 M potassium cyanide was then added. The solution was mixed and allowed to react on ice for 5 minutes. For samples with lower amounts of thiosulfate, up to 0.5 mL was used; the volume of milli-q water added in the first step was adjusted accordingly.

(2) 0.6 mL of a 0.1 M copper sulfate solution was added, the solution was mixed and allowed to react on ice for 10 minutes.

(3) 1.2 mL of a ferric nitrate reagent (304 g iron (III) nitrate and 100 mL 65% nitric acid, brought up to 500 mL with milli-q water) and 2.2 mL anoxic milli-q water were added, the solution was mixed and allowed to react at room temperature and in the dark for 25 minutes.

(4) Absorbance was measured at 460 nm and compared to the calibration curve.

Anion chromatography

Lactate and acetate concentrations were determined on 0.45 μm filtered sampled suppressed anion chromatography with conductivity detection using an eluent gradient method (ICS-2000, AS11 column, Dionex). First, 1 mM KOH was run isocratically for 6 min followed by an initial linear ramp to 30 mM over 8 min and a

final linear ramp to 60 mM over 4 min, allowing to re-equilibrate at 1 mM KOH between samples (run in duplicates).

Sample preparation for isotopic analysis

Each sulfur pool of interest was separated and purified prior to isotopic analysis. The procedure is similar to that described in Smock et al (1998).

Samples containing sulfide (in the form of zinc sulfide), aqueous sulfite and thiosulfate were centrifuged at maximum speed for 15 minutes. The pellet (zinc sulfide) was washed and centrifuged with milli-q twice before performing an Acid Volatile Sulfur extraction (AVS extraction), allowing extraction of S^{2-}, followed by a Chromium Reducible Sulfur extraction (CRS extraction), retrieving zero valence sulfur. The supernatant (containing sulfite and thiosulfate) was combined with a 0.3 M $BaNO_3$ solution (added in excess of sulfite) and allowed to react for at least 3 hours. The $BaSO_3$ precipitate was recovered via filtration or centrifugation. It was then oxidized to $BaSO_4$ by combining it with excess 30% hydrogen peroxide. The mixture was allowed to react overnight at 50°C. The sulfur in the resulting sulfate (as $BaSO_4$) was then extracted via a thode extraction procedure.

Thiosulfate (found in the remaining liquid phase) was decomposed to Ag_2S (sulfane group) and $BaSO_4$ (sulfonate group) (see figure 19 for a molecular structure indicating these two groups) by first adding a 4 M solution of $AgNO_3$ in excess of all anions present in solution (including thiosulfate) followed by the 0.3 M $BaNO_3$ in excess of thiosulfate (Smock et al, 1998). The resulting solution (containing a precipitate composed of Ag_2S, $BaSO_4$ and other silver and barium precipitates) was allowed to react overnight in the dark at 50°C and filtered out. All sulfur was extracted by first performing an AVS extraction (extracting Ag_2S, thus the sulfane group), followed by a thode extraction (extracting $BaSO_4$, the sulfanate group) and a CRS extraction (extracting any leftover elemental sulfur).

Equations

Kinetics of bacterial growth

Doubling times in batch cultures were determined using the definition described in Lenski et al (1991):

$$d = \frac{ln\left({}^{N_2}/_{N_1}\right)}{\ln(2)} \qquad (13)$$

Where N_1 is the number of bacteria (or corresponding optical densities) at the start of mid-log phase and N_2 being the number of bacteria (or optical densities) at the end of mid-log. This gives the number of doublings across the time interval of mid-log phase, which can be extrapolated over 24 hours thus giving the number of doublings per day.

Chemostat

The dilution rate (in units of day^{-1}) of the chemostat was calculated as following:

$$D = \frac{rate\ of\ outflowing\ liquid}{reactor\ final\ volume} \qquad (14)$$

The rate of outflowing liquid is in L/day and the reactor final volume in L. This means that the mean residence time of any particle in the reactor is equal to 1/D (in units of days).

Mass balance

Mass balance in batch conditions was calculated by determining the total moles of sulfur contributed by each species for each time point.

Sulfite and sulfide were considered to contribute only one mole of sulfur per mole of sulfite or sulfide. Thiosulfate, on the other hand, was considered to contribute two moles of sulfur per mole of thiosulfate.

$$S_{total} = V_{culture}[SO_3^{2-}]_{culture} + V_{culture}[H_2S]_{culture} + 2V_{culture}[S_2O_3^{2-}]_{culture} \quad (15)$$

Mass balance was considered to be closed if the total moles of sulfur in culture was found to be constant, within error, and equal to the initial moles of sulfur (sulfite only) throughout the course of the experiment.

In continuous culture, sulfur balance was determined by comparing the flow of moles of sulfur entering the reactor and the flow of moles of sulfur leaving the reactor. The flux of sulfur going into the reactor was calculated based on the sulfite concentration of the batch media reservoir and the measured rate of media flowing into the reactor.

$$S_{in} = v_{in}[SO_3^{2-}]_{in} \quad (16)$$

As for the flux of sulfur leaving the reactor, it was determined based on the measured rate of media flowing out of the reactor and the concentration of sulfite and thiosulfate measured in the liquid trap, and sulfide in the gas trap.

$$S_{out} = v_{out}[SO_3^{2-}]_{liquid} + v_{out}[H_2S]_{gas} + 2\,v_{out}[S_2O_3^{2-}]_{liquid} \quad (17)$$

Balance was reached when the rate of incoming sulfur equalized the rate of outgoing sulfur.

Error propagation

For equation 15:

$$\sigma_{S_{total}} = \sqrt{\left(V_{culture}\sigma_{[SO_3^{2-}]}\right)^2 + \left(V_{culture}\sigma_{[S^{2-}]}\right)^2 + \left(V_{culture}\sigma_{[S_2O_3^{2-}]}\right)^2} \qquad (18)$$

For equation 16:

$$\sigma_{S_{in}} = \upsilon_{in}\sigma_{[SO_3^{2-}]_{in}} \qquad (19)$$

For equation 17:

$$\sigma_{S_{out}} = \sqrt{\left(\upsilon_{out}\sigma_{[SO_3^{2-}]_{liquid}}\right)^2 + \left(\upsilon_{out}\sigma_{[S^{2-}]_{gas}}\right)^2 + \left(2\upsilon_{out}\sigma_{[S_2O_3^{2-}]_{liquid}}\right)^2} \qquad (20)$$

For the isotopic difference between two pools:

$$\sigma_{\delta^{34}S_B - \delta^{34}S_A} = \sqrt{\left(\sigma_{\delta^{34}S_A}\right)^2 + \left(\sigma_{\delta^{34}S_B}\right)^2} \qquad (21)$$

For equation 7, the error propagation found in Johnston et al (2007) was used.

Results

Batch experiment

The batch experiment was run for over 114 hours. OD_{600} levels increased from 0.129 after inoculation (background OD_{600} = 0.004) to 0.902.

Sulfite concentrations decreased regularly from 71.58 to 25.47 mM. Concomitantly, sulfide concentrations increased from 0.07 mM to a peak of 13.97 mM and decreasing to 6.21 mM at the end of the experiment. Thiosulfate concentrations increased from 0.59 to 18.55 mM. All reported values are averages across triplicate experiments. Initial values correspond to concentrations after medium inoculation, background levels were effectively zero. See figure 1 for the evolution of the abundance of sulfite, sulfide and thiosulfate, and optical densities over the course of the experiment.

The sulfite and sulfide phases did not show large changes in neither major nor minor isotopic abundances. Sulfite's $\delta^{34}S$ values evolved from an initial 0.073 ‰ to a final value of -0.057 ‰. Sulfide presented a slight increase from $\delta^{34}S$ values of -9.13 to -8.13 ‰. Thiosulfate presented a large site-specific isotopic offset that increased over the course of the experiment. The sulfane's $\delta^{34}S$ values decreased from -4.86 to -7.19 ‰ while sulfonate increased from 12.33 to 21.19 ‰. These reported values are averages across triplicates. Tables 1, 2 and 3 show the major and minor isotopic compositions of the individual triplicate lines.

Extracts were obtained from CRS extractions from only the sulfide phase. These were depleted in ^{34}S, and showed very little change in major and minor isotopic compositions over the course of the experiment. Initial $\delta^{34}S$ values averaged to -10.43 ‰ across triplicates. Final values averaged to -9.45 ‰. Table 4 below presents the major and minor isotopic abundances characterizing this extract in the three triplicate lines.

Chemostat experiment

The chemostat experiment was run for 485 hours. At 405 hours, all measured variables became constant and were maintained for the following 80 hours. The reactor's final volume was 0.5 L. The rate of outflowing medium from the reactor averaged to 0.189 L/d. Optical densities and pH stabilized to 0.083 and 7.171 respectively (figure 2). Lactate concentrations in the reactor were effectively zero. Conversely, acetate levels averaged to 7.89 mM (figure 3). Sulfite concentrations of the inflowing medium, the reactor and the liquid trap were 20.51, 16.45 and 15.56 mM respectively. Most of the sulfide produced accumulated in the gas trap, its concentrations to averaging 9.81 mM. The concentration of thiosulfate in the reactor and the liquid trap were 0.51 and 0.38 mM (figures 4, 5 and 6).

Between 405 and 485 hours, the isotopic composition of sulfide, sulfite and thiosulfate were constant. The sulfide and sulfite $\delta^{34}S$ values averaged to -15.17 and 0.67 ‰ respectively. Thiosulfate presented a large site-specific isotopic offset: sulfane's $\delta^{34}S$ averaged to -33.89 ‰ while sulfonate's values were 7.38 ‰. Table 5 below shows a summary of the major and minor isotopic composition of sulfide, sulfite and thiosulfate.

No extract was obtained from CRS extractions of neither the sulfide nor the thiosulfate phases.

Abiotic experiment

In two of the four experiments, thiosulfate production was concomitant with sulfide consumption. The highest levels of thiosulfate were observed with intermediate initial sulfide concentrations: for initial sulfide concentrations of 6.59 and 11.95 mM, thiosulfate concentrations reached 6.59 and 5.32 mM. The other two lines, in which initial sulfide concentrations were 0.06 and 17.89 mM, thiosulfate production was limited: 0.09 and 1.51 mM respectively. Figures 7 and 8 show the change in sulfide and thiosulfate concentrations over the course of the abiotic experiment. The sulfite assay yielded highly variable results and no decreasing trend as would be expected given the diminishing sulfide levels and corresponding increasing thiosulfate levels.

Analysis

Batch experiment

Sulfur compounds: abundance and evolution over the course of the experiment

OD_{600} levels, sulfite, sulfide and thiosulfate concentrations decreased and cease to change to become steady 29.75 hours after inoculation of the medium, indicating that the bacteria reached stationary phase and, subsequently, all lactate available (present in limiting concentrations) had been consumed. The total sulfur content was constant throughout the course of the experiment, averaging to 70.29 mM, effectively closing mass balance (figure 9).

The first question that needs addressing concerns the biochemistry of the metabolic pathway of JW9021. This includes identifying the reactants, the products, and their corresponding stoichiometry. The total moles of sulfite consumed and of

sulfide and thiosulfate produced over the course of the exponential phase (between 0 and 29.75 hours) are summarized table 6. For sulfite, the moles consumed were calculated by subtracting the total moles in solution at the end of exponential phase to the total moles at the start of the phase. Conversely, for sulfide and thiosulfate, the moles produced are determined by subtracting the total moles at the start of the exponential phase (after medium inoculation) to the total moles at the end of the phase. These are then used to determine the stoichiometric coefficients of the sulfur compounds involved in the reduction of sulfite to sulfide (for each triplicate line, see table 7). This was done by dividing the moles of sulfide or thiosulfate produced by the moles of sulfite consumed.

Comparing this stoichiometry to the one observed in the chemostat experiment will provide with a better understanding of the reaction sequence that is taking place. To facilitate this comparison, only rates will be compared. The rates of sulfite consumption and sulfide and thiosulfate production during exponential phase were calculated by determining the slope of the decrease or increase of the levels of each sulfur species as a function of time. These rates are summarized in the table 8 (for all triplicate lines) in units of moles per hour.

The extract obtained during the CRS extraction performed on the sulfide phase is postulated to correspond to a small pool of elemental sulfur that accumulated in the medium. An AVS extraction was always performed on the zinc sulfide precipitate, which was always present in amounts small enough to ensure full reaction and subsequent extraction of the S^{2-}. Therefore, it is improbable that this extract corresponds to left-over sulfide.

Isotopic abundance

Figure 10, 11 and 12 (triplicates 1, 2 and 3 respectively) show the evolution of the isotopic composition, expressed as $\delta^{34}S$, in units of ‰, of sulfite, sulfide and the sulfane and sulfonate groups of thiosulfate as a sulfite is being consumed. The latter is expressed as the fraction *f* of the total sulfur in solution that corresponds to

sulfite. It will be noted that *f* does not decrease below 0.4, because, in this experiment, lactate, and not sulfite, was limiting. Therefore, sulfite reduction did not carry on until full sulfite depletion. All values correspond to samples taken over the course of the exponential phase only. The isotopic composition of the CRS extract, thereby referred to as elemental sulfur, is also shown. Figure 13 shows the data for all triplicates. The small variation in isotopic composition of sulfite and sulfide as f decreases is unexpected, especially given the large site-specific (sulfane and sulfonate) isotopic offset in thiosulfate.

The value of $\Delta^{33}S$ at each point is calculated using the reported $\delta^{34}S$ and $\delta^{33}S$ and the equation depicted previously. See table 9 for a full summary of these values across triplicate lines. The average $\Delta^{33}S$ of each data point was plotted as a function of its corresponding $\delta^{34}S$. Both were weighed by the fraction of the total sulfur each phase represents. These values were also modified so that the isotopic composition of the initial sulfite fell at the (0, 0) coordinates. Figure 14 presents said plot for the sulfide, sulfide, sulfonate and sulfane phases. A "mixing" component corresponding to the sum in $\delta^{34}S$ and $\Delta^{33}S$ of each phase was also included in the plot.

The "mixing" component falls within the vicinity of the initial sulfite's isotopic composition. The missing sulfur would potentially correspond to the elemental sulfur found with the sulfide phase, for which no concentration data was available, and thus was not included in the plot itself. The fraction of elemental sulfur can be deduced using the following relationship, *m* corresponds to the total moles of each particular sulfur pool:

$$m_{elemental} = \frac{\delta^{34}S_{SO3i}m_{SO3i} - \left(\delta^{34}S_{SO3}m_{SO3} + \delta^{34}S_{H2S}m_{H2S} + \delta^{34}S_{sulfane}m_{sulfane} + \delta^{34}S_{sulfonate}m_{sulfonate}\right)}{\delta^{34}S_{elemental}} \quad (22)$$

The amount of elemental sulfur for each triplicate is summarized in table 10. These, and the corresponding isotopic composition, are then treated in the same manner as explained earlier and included into the analysis of isotopic balance. The value bearing a negative sign was excluded from this analysis. The new "mixing" component is shown to fall closer to the isotopic composition of the initial sulfite.

Chemostat experiment

Steady state

The maintenance of constant optical densities, pH, acetate, sulfite, sulfide and thiosulfate concentrations, together with the absence of lactate in the reactor confirm that steady state was maintained between 405 and 485 hours.

The average rates of sulfite consumption and sulfide and thiosulfate production during steady state are summarized in table 11. Similarly to the treatment given to the batch experiment's rates of consumption and production, these are used to determine the stoichiometric coefficients of each sulfur species (see table 12). The reported rates are shown in more detail figure 15, which depicts the rates of sulfite going into the reactor and sulfite, sulfide and thiosulfate leaving the reactor per sampling point. The rates of total sulfur entering and leaving the reactor are also shown. The rates of inflowing and outflowing medium were within error of each other, effectively closing sulfur flow balance. This further supports the fact that the system has reached steady state and allows performing isotopic analyses on each sulfur species.

Isotopic analysis

The isotopic composition of sulfite, sulfide, sulfane and sulfonate was constant during the time interval during which steady state was maintained, as shown in figure 16, in which the isotopic abundance of the sulfur compounds is expressed as $\delta^{34}S$, in units of ‰.

The isotopic composition of the sulfur entering the reactor was compared to the isotopic composition of the sulfur leaving it. This was done by comparing the $\delta^{34}S$ of the inflowing sulfite weighed by the incoming flux and the sum of the $\delta^{34}S$ weighed by the outgoing flux of each sulfur species (see figure 17). The isotopic composition of inflowing and outflowing sulfur fell in close vicinity, therefore closing isotopic flow balance.

Chemostat experiments mimic open systems and thus allow determining the fractionation factor without having to apply Rayleigh distillation models. The fractionation factor for both major ($^{34}\alpha$) and minor ($^{33}\alpha$) isotopes between reactant and product were therefore calculated using equation 9. Since both sulfide and thiosulfate were identified as products of sulfite reduction, fractionation factors using either sulfide or thiosulfate as first product are calculated and compared (see table 13 and 14).

Abiotic experiment

Sulfide consumption was concomitant to thiosulfate production. Rates of sulfide consumption and thiosulfate production were calculated by zooming into the "exponential phase" of each curve (between 0 and 74 hours for all) and determining the slope of the line obtained. The rate at which sulfide depleted equaled the rate at which thiosulfate was produced but with opposite signs (see table 15).

This experiment was run with sulfide under the form of sodium sulfide nonanhydrate. This compound is known to cause a significant pH shift when dissolved. Indeed, the dissolution reaction of sodium sulfide nonanhydrate is as following:

$$Na_2S + H_2O \rightarrow HS^- + OH^- + 2Na^+$$

In this experiment, thiosulfate production increased when the initial sulfide concentration is raised from 0 to 6.59 mM. Further increase of the concentration of sulfide was associated with lesser extents of thiosulfate production. Higher concentrations of initial sulfide lead to a more extreme pH shift. This is consistent with the results obtained by Heunisch (1977). In this study, the author observed an important decrease in the amount of thiosulfate produced at pH's higher than 7.50.

This pH shift would explain the unexpected lack of decreasing trend and high noise observed in the sulfite concentration results. The fuschin assay relies on the reaction of the complex composed of pararosaniline hydrochloride and sulfuric acid with formaldehyde. The solution then further reacts with sulfite under the form of bisulfite (Grant, 1947; Steigmann, 1942). Hence, this reaction is pH sensitive, and any shifts from neutral pH's compromise the reproducibility of the reaction.

Because of this, the sulfite concentration is deduced based on the concentrations of sulfide and thiosulfate. The production of one mole of thiosulfate requires one mole of sulfide and one mole of sulfite, as obvious in the rates of thiosulfate production and sulfide consumption: they have equal absolute values but are of opposite signs. Thus, for each mole of sulfide consumed, one mole of sulfite is consumed as well. Therefore:

$$[SO_3^{2-}]_{t1} = [SO_3^{2-}]_{t0} - ([S^{2-}]_{t0} - [S^{2-}]_{t1}) \qquad (23)$$

At t_0 the sulfite concentration used corresponded to the levels measured in the control line (averaged to 35.90 mM). The resulting sulfite concentrations for each line are summarized in figure 18.

Comparing these rates of thiosulfate production and sulfite and sulfide consumption with those observed in both the batch and chemostat experiments allows estimating the contribution of this reaction to the overall thiosulfate pool. If this inorganic reaction has a significant effect on the abundance of different sulfur species, it might also have an effect on their isotopic composition. The contribution of this reaction to the sulfur isotope abundances of sulfite, sulfide and thiosulfate will also be analyzed and, if possible, quantified.

Interpretation

Biochemistry

In both the batch and chemostat experiments, sulfite consumption was concomitant with the production of thiosulfate and sulfide. These compounds have been observed to accumulate during the reduction of sulfite by sulfate reducing bacteria and enzyme extracts in previous studies supporting the trithionate pathway, or a version of it (Findley and Akagi, 1969, 1970; Lee, 1971; Kobayashi et al, 1969, 1972; Vainshtein, 1980; Fitz and Cypionka, 1990 and Sass, 1992). Therefore, it would be logical to conclude that the reaction network of this bacterium's metabolism includes the production of thiosulfate as an intermediate, ultimately reduced to sulfide.

However, the results from the abiotic experiment have shown that thiosulfate can be produced from the inorganic reaction of sulfite and sulfide. It follows that at least part of the thiosulfate observed in either batch or continuous culture experiments (or both) is, at least in part, produced inorganically. It is therefore crucial to be able to differentiate between the two thiosulfate-forming processes (abiotic versus biotic) and understand their relative contribution to the final thiosulfate pool.

This can be done by analyzing the rates of sulfite consumption, and of sulfide and thiosulfate production in both experiments. Net rates result from two fluxes: a biotic and an abiotic flux. This is expressed in the following equations:

$$\frac{d[S_2O_3^{2-}]}{dt} = v_{abiotic} + x \qquad (24)$$

$$\frac{d[SO_3^{2-}]}{dt} = -v_{\beta} - \frac{1}{2}v_{abiotic} \qquad (25)$$

$$\frac{d[S^{2-}]}{dt} = v_{\beta} - \frac{1}{2}v_{abiotic} \qquad (26)$$

Where $\upsilon_{abiotic}$ is the rate of consumption or production of sulfur species due to abiotic effects. The abiotic experiment has shown that for each mole of sulfite and each mole of sulfide reacting, one mole of thiosulfate is produced. Therefore, the abiotic flux is, here, assumed to bear a positive sign for thiosulfate and be halved and bear a negative sign for sulfite and sulfide. Conversely, υ_B is the rate of consumption or production of sulfur compounds due to biological activity. Bacteria consume sulfite and produce sulfide, which is why a negative sign was attributed to the biotic effect in the sulfite equation, and a positive sign in the sulfide equation. Since one mole of sulfide is produced for each mole of sulfide, the same rate was given for both of them. Finally, the component "x" represents the net effect of biotic processes on the thiosulfate levels observed. Because the role of thiosulfate in the reduction of sulfite is, in this metabolism, unclear, it is assumed that the net biotic process contributing to the thiosulfate pool is different from the biotic effect of sulfite consumption and sulfide production. No assumption is made regarding the sign of this term.

From the rates measured in the batch experiment (all values are in units of moles per hour):

$$\frac{d[SO_3^{2-}]}{dt} = -6.92x10^{-5}$$

$$\frac{d[S^{2-}]}{dt} = 2.34x10^{-5}$$

$$\frac{d[S_2O_3^{2-}]}{dt} = 2.54x10^{-5}$$

Therefore, the above equations can be expressed as:

$$-v_\beta - \frac{1}{2}v_{abiotic} = -6.92x10^{-5}$$

$$v_\beta - \frac{1}{2}v_{abiotic} = 2.34x10^{-5}$$

$$v_{abiotic} + x = 2.54x10^{-5}$$

By adding the first two equations and solving for $\upsilon_{abiotic}$:

$$v_{abiotic} = 4.58x10^{-5}$$

And thus, the rate of biotic formation of thiosulfate becomes:

$$x = 2.54x10^{-5} - v_{abiotic}$$

$$x = -2.04x10^{-5}$$

If the same calculations are performed for the chemostat experiment, given the rates observed, the following values are obtained:

$$v_{abiotic} = 3.33x10^{-6}$$

$$x = 0$$

The rate of inorganic thiosulfate formation is one order of magnitude higher in the batch experiment than in the chemostat. The experimental design of the chemostat involved the prompt removal of sulfide from the reactor (evident in the low concentrations observed in both the reactor and the outflowing medium), therefore limiting the extent of the inorganic reaction between sulfite and sulfide. In batch, the net flux of thiosulfate due to biological effects is 45% of the abiotic flux. Most importantly, it bears a negative sign. This means a net consumption of inorganic thiosulfate by the bacteria as it is produced. The rate of net thiosulfate production due to biological effects is estimated to be near zero in the chemostat. This implies that all thiosulfate observed in this system is inorganic.

There is, as a consequence, only evidence for extracellular thiosulfate accumulation resulting from the inorganic reaction between sulfite and sulfide. This is further supported by the presence of elemental sulfur in the batch. Indeed, studies by Barbieri and Majorca (1960) and Neiman et al (1952) have shown that the inorganic reaction producing thiosulfate also produces elemental sulfur as an intermediate. In their experiments, they followed the fate of ^{35}S labeled sulfide and observed the accumulation of labeled zero valence sulfur as the reaction proceeded. This would explain the origin of the elemental sulfur observed in the batch experiment, which bears a strikingly similar isotopic composition (in both the major and the minor sulfur isotopes) to the sulfide phase. This is consistent with the fact that sulfide reduction to zero valence sulfur bears little to no isotopic effect (Fry et al, 1986; Habicht et al, 1998).

It could be argued that thiosulfate arose from a parallel and independent reaction. In this case, the direct reduction of sulfite to sulfide occurs in parallel to the reduction of sulfite to thiosulfate. However, this would require a rate of sulfite reduction three times larger than the rates of either sulfide or thiosulfate production. These are not met in the current study.

Despite this conclusion, the potential for thiosulfate to be an intermediate of sulfite reduction cannot be completely excluded. Both experiments were run under excess sulfite conditions, which promote the accumulation of intracellular sulfur intermediates. Resolving this issue requires either following the fate of sulfur as it travels through the reaction pathway or measuring the intracellular levels of this intermediate redox species, as well as the sulfur species produced by enzyme extracts alone. Chambers and Trudinger (1975) used ^{35}S labeled sulfate and thiosulfate to show that the latter was not an intermediate species of sulfite reduction. However, all that was shown indubitably was that the sulfane and sulfonates groups were reduced at the same rate. Additionally, the authors showed that thiosulfate is actively exchanged between the intracellular and the extracellular environments. This supports the negative biotic flux of thiosulfate, postulated to represent the utilization of this intermediate species by the bacteria. It follows that the bacteria probably possess the protein machinery necessary for the reduction of thiosulfate.

The fact that the bacteria were found to utilize inorganic thiosulfate in the batch and not the chemostat would result from the extent of accumulation of this species, which accumulated to higher levels in the batch than the chemostat. Experiments using cell and enzyme extracts have shown that both trithionate and thiosulfate are produced as a result of sulfite reduction (Findley and Akagi, 1969; Kobayashi et al, 1969, 1972). More sophisticated enzyme experiments looking into the species produced by purified enzyme extracts confirmed this (Oliveira et al, 2008; Parey et al, 2010; Drake and Akagi, 1977; Peck et al, 1982; Haschke and Campbell, 1971; Aketagawa et al, 1985; Hatchikian, 1975). The most recent enzyme experiment analyzing the reduction of sulfite by DsrAB (Leavitt et al, personal communication) showed that the reduction of sulfite led to the production of

thiosulfate and trithionate, but not sulfide. Fitz and Cypionka (1990) argued that trithionate acts as a strong oxidizing agent and is therefore reduced immediately to thiosulfate. This explains why it might not accumulate to detectable levels in experiment using bacterial cultures. Therefore, the possibility for trithionate to also be produced by this bacterium is not excluded either.

Although complementary, comparing bacterial and enzyme extract experiments must be done with caution. The former allows exploring the effect of specific factors on the overall metabolic machinery. The repercussions on the bacterial community and hence the consequences of the metabolism's influence on the environment can be extrapolated. This is not possible in enzyme experiments, which focus solely on the reaction catalyzed by a given enzyme. This approach, on the other hand, allows exploring the mechanisms by which said reaction occurs and the specific factors affecting. Plus, it enables eliminating the effect of other rate-limiting steps, which is not possible in bacterial culture experiments.

Consequently, suggesting a metabolic pathway that is fully supported by the results obtained in both the batch and chemostat experiments is challenging. A number of models will, nevertheless, be proposed.

In the first case-scenario, sulfite is reduced directly to sulfide. Neither thiosulfate nor elemental sulfur are intermediates of the metabolic pathway but result from the inorganic reaction of sulfite and sulfide. The bacteria would potentially utilize this inorganic thiosulfate. This model accounts for the analysis and interpretation of the sulfur species levels observed but is not supported by the literature cited earlier. In the second case-scenario, thiosulfate is an intermediate species of sulfite reduction. Inorganic thiosulfate and elemental sulfur would still accumulate in the medium and the bacteria would potentially utilize thiosulfate. In the third case-scenario, trithionate and thiosulfate are intermediate species of the metabolic pathway. Additional thiosulfate and elemental sulfur would be produced inorganically. The bacteria would utilize this inorganic thiosulfate.

Fractionation factor

Despite net sulfite consumption and sulfide production, the corresponding isotopic composition presented a very slight change over the course of the batch experiment. This system's isotopic character is hence quite unique, as it does not behave as a classical closed system where DSR is the only process fractionating sulfur isotopes. If this were the case, there would be a net enrichment of both sulfite and sulfide. The lack of change in either of them suggests that more than one process is at play. Since this bacterium's mutation hinders the possibility for sulfite disproportionation (Zane et al, 2010; Johnston et al, 2007) and sulfide oxidation likely does not occur (all precautions were taken to maintain the system as reducing and anaerobic as possible), it follows that the inorganic production of thiosulfate and/or its utilization by the bacteria were these additional processes. As a consequence of this complicated reaction network a fractionation factor for just the sulfite to sulfide step in the batch experiment cannot be estimated. The net fractionation, however, was -8.26 ‰ and results from the combined isotopic effects of each process weighed by the flux of sulfur between pools.

In the chemostat experiment, sulfite presented a similar extent of enrichment as in the batch experiment. Sulfide, however, was far more depleted. The extent of inorganic reactions occurred to a lesser extent than in the batch experiment. Additionally, it was postulated that the bacteria likely did not consume abiotically produced thiosulfate. As a result, the reaction network in this experiment is simpler than in the batch. The net fractionation produced by the sulfite to sulfide reduction by the bacteria can thus be estimated: -15.88 ‰ over the course of steady state. Incorporating this into the Rees model gives an upper fractionation limit for DSR of -37.88 ‰.

The largest isotopic change, in both the batch and chemostat experiments, was observed for the thiosulfate pool. In the batch experiment, the bulk composition of thiosulfate averaged to 1.66 ‰ and presented a slight enrichment of 2.14 ‰ over the course of the exponential phase. The site-specific isotopic composition of

thiosulfate, however, presented a significant offset, averaging to 29.74 ‰ and increasing by 13.43 ‰ by the end of the exponential phase. The sulfane and sulfonate groups in the thiosulfate produced in the chemostat also presented a significant isotopic offset of 41.27 ‰.

The small enrichment of the thiosulfate bulk isotopic composition, combined with the large site-specific offset, was observed in previous studies. Habicht et al (1998) measured the isotopic abundance of sulfide and thiosulfate sulfane and sulfonate as *D. salexigens* reduced thiosulfate. The authors observed a significant thiosulfate site-specific isotopic offset, although the sulfane group became more enriched while, in the current study, this site became more depleted. Also, *D. salexigens* was grown only in the presence of thiosulfate, without coexistence of aqueous sulfite and sulfide, and thus any change in isotopic composition of this phase resulted exclusively from bacterial growth. Cummins et al (2013, in press) observed a similar offset in the site-specific isotopic composition of thiosulfate when growing *D. alaskensis* (strain G-20) as either a sulfite or a thiosulfate reducer. This study involved the co-existence of aqueous sulfide and sulfite; part of the observed thiosulfate could thus be of inorganic origin as well.

The site-specific offset was found to increase over the course of the experiment. In enzyme experiments (Leavitt et al, personal communication), the thiosulfate produced during the reduction of sulfite by DsrAB also presented a large site-specific isotopic offset. Because of the uniqueness of this mutant's metabolic pathway, it is difficult to make direct comparisons between the present study and other experiments. However, the common observations between these experiments points towards a common mechanism causing this general trend.

The large site-specific isotopic offset could be explained via the difference in bonding environments of the sulfane and sulfonate groups. The former is reduced while the latter is, conversely, oxidized. A large difference in their corresponding isotopic composition would therefore be expected, but the mechanism causing this (whether it is of biotic or abiotic origins) is unclear. Similar offsets were observed by Chambers and Trudinger (1979), who observed a difference of 14 ‰ between the sulfane and the sulfonate groups of thiosulfate resulting from the chemical

reaction of aqueous sulfide and sulfite. The authors did not, however, suggest a mechanism explaining this observation. In the current study, this offset was larger in the chemostat than in the batch experiment. Therefore, at least for the inorganically produced thiosulfate, the inherent differences between the two experiments likely affected the degree of the site-specific isotopic offset. It is unclear what specific factor (pH, concentration of aqueous sulfite and sulfide, the presence of bacteria likely consuming thiosulfate) has the primary effect.

Because of the complicated chemistry occurring in the batch experiment, it is suggested that additional rates (lower and higher than 10% maximum growth) have to be analyzed in the chemostat in order to understand the behavior of $^{34}\varepsilon$ and $^{33}\lambda$ as a function of growth rate.

Conclusion

The sulfite reduction step is the least understood reaction of the DSR metabolic pathway. The most widely accepted model describing the fractionation of sulfur isotopes, the Rees model (1973), heavily relies on the unidirectionality of this reaction to assign it a theoretical isotopic effect of -25 ‰. However, a vast array of experiments has shown that the reduction of sulfite likely occurs in a multi-step fashion (Findley and Akagi, 1969, 1970; Lee, 1971; Kobayashi et al, 1969, 1972; Vainshtein, 1980; Fitz and Cypionka, 1990 and Sass, 1992) and that the assigned isotopic effect might be in the lower limit of possibilities (Rees, 1973; Brunner and Bernasconi, 2005; Johnston et al, 2007). Because of the reversibility of this reaction and the capacity of SRB's to disproportionate sulfite, this issue has, to date, not been possible to address. The present study makes use of a strain of *D. vulgaris* Hildenborough with a unique mutation that effectively isolates the sulfite reduction step from the rest of the metabolism and hinders the possibility for disproportionation.

A definite model for the biochemistry of sulfite reduction in this bacterium could not be proposed. Although both sulfide and thiosulfate were produced as sulfite was consumed, the simultaneous occurrence of biotic and inorganic reactions rendered the identification of fluxes between pools and thus the network's structure challenging. Additionally, in the batch experiment, the isotopic composition of every sulfur pool did not behave as a classic closed system Rayleigh model (Canfield, 2001). Therefore, for this experiment, a specific net fractionation factor could not be calculated for the closed system experiment. The chemostat experiment, on the other hand, allowed estimating a net fractionation factor between sulfite and sulfide of -15.88 ‰. This value falls within the range of previously reported fractionation factors measured when growing SRB's on sulfite (Kemp and Thode, 1968), but is in the lower limit of possibilities suggested by theoretical models (Rees, 1973; Brunner and Bernasconi, 2005; Johnston et al, 2007). The resulting upper fractionation limit for DSR fails to explain the large range of fractionations observed in natural settings (Ohmoto et al, 1990; Brunner and Bernasconi, 2005; Wortmann et al, 2001; Rudnicki et al, 2001; Claypool, 2004; Neretin et al, 2003). It must be stressed that this chemostat experiment was run at 10% maximum growth rate. Consistent with the rate-dependence of sulfur isotope fractionation by SRB's, a wider range of fractionations is expected as additional rates are explored (Chambers and Trudinger, 1975; Sim et al, 2011; Leavitt et al, 2013).

The strong isotopic offset between the sulfane and sulfonate groups in thiosulfate might, in this study, not necessarily derive from a biological effect. The difference in oxidation states between the two sites indicates that the large isotopic offset is not a striking observation, however, the mechanism by which this would occur inorganically is unclear. The fact that the same trend was observed in past abiotic (Chambers and Trudinger, 1979) and biotic in vivo and in vitro experiments (Habicht et al, 1998; Cummins et al, 2013, in press; Leavitt et al, personal communication) suggests a mechanism common to the inorganic and enzyme-catalyzed reactions. It is crucial to fully understand the mechanisms of the inorganic and enzyme-catalyzed thiosulfate forming reaction and differentiate between the

two reactions. For this, a more exhaustive experiment analyzing the inorganic reaction (rates of reaction and isotopic composition) and the factors affecting it (such as pH and reagent concentration) must be run.

The extensive production of inorganic thiosulfate during both experiments indicates that this reaction likely occurs in both laboratory and environmental settings. In addition, it probably bears a specific isotopic effect. This calls for caution when using sulfur species abundances and isotopic composition during sulfite reduction experiments to establish metabolic networks and fractionation factors, as this reaction most likely affects the reaction network and isotopic composition of the sulfite, sulfide and thiosulfate pools.

The current study has provided with unique insight into the most debated upon step of microbial sulfate reduction. The results, interpretation and comparison of batch and chemostat experiments have arisen more questions than answers. The conclusions that can be drawn with certainty include: (1) the fractionation factor of sulfite reduction is likely around 16 ‰ for the rates and the environment of the experiment described here; and (2) the thiosulfate that was found to accumulate in the extracellular environment is likely inorganic and cannot be included in the biochemistry and the isotopic analysis. Further analysis of this bacterium's activity, combined with analysis of the activity of the enzyme's involved in this step and the abiotic reaction forming thiosulfate, will provide with a clearer picture of sulfite reduction, its mechanism, the factors affecting it and the implications for the upper fractionation limit of DSR.

Figures and Tables

Figures

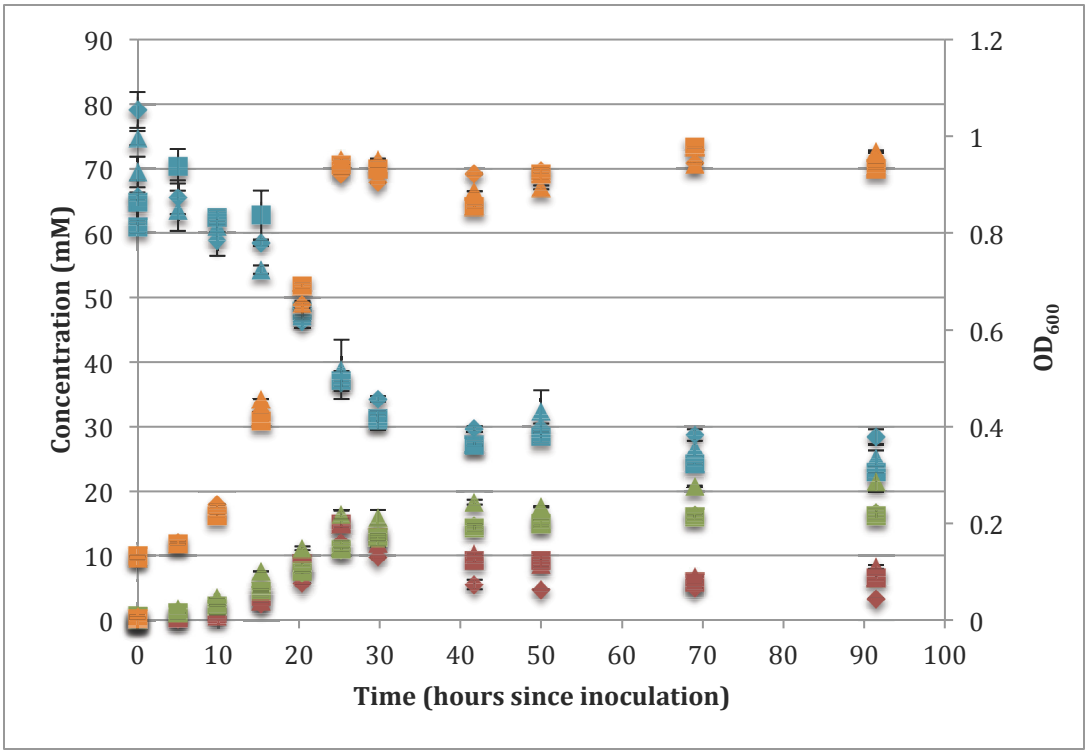

Figure 1: Optical densities (orange) and total moles in culture of sulfite (blue), sulfide (red) and thiosulfate (green) as a function of time. Data for triplicates 1 (diamonds), 2 (squares) and 3 (triangles) are shown. Error bars shown correspond to 1 SD.

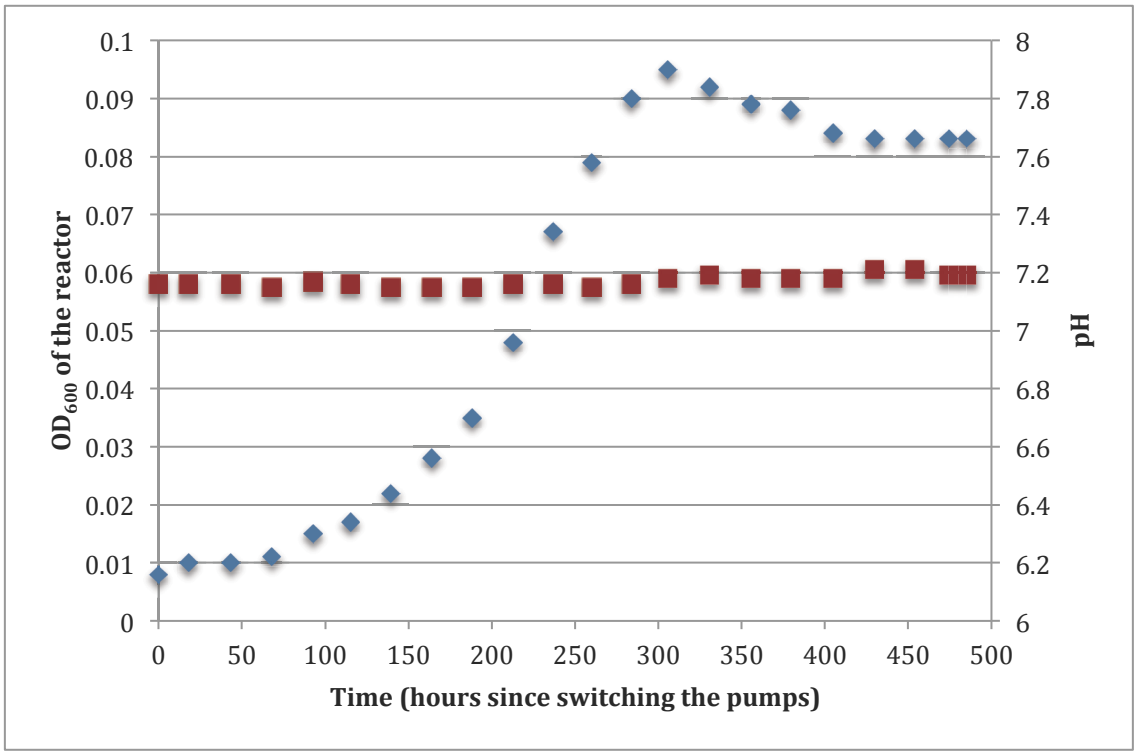

Figure 2: Optical densities (blue diamonds) and pH levels (red squares) throughout the chemostat run.

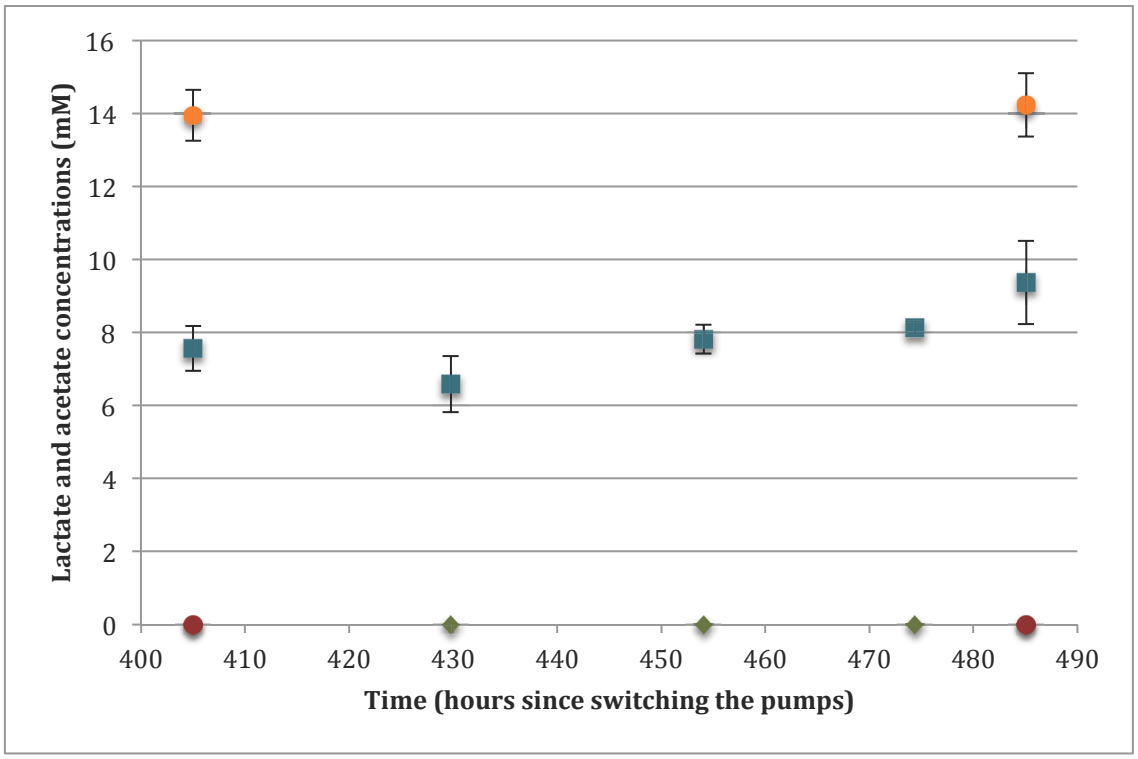

Figure 3: Lactate (green diamonds) and acetate (blue squares) concentrations in the reactor through the steady state time interval. Lactate and acetate concentrations in the reservoir media batch (orange circles and red circles respectively) are shown as reference. Error bars correspond to 1 SD.

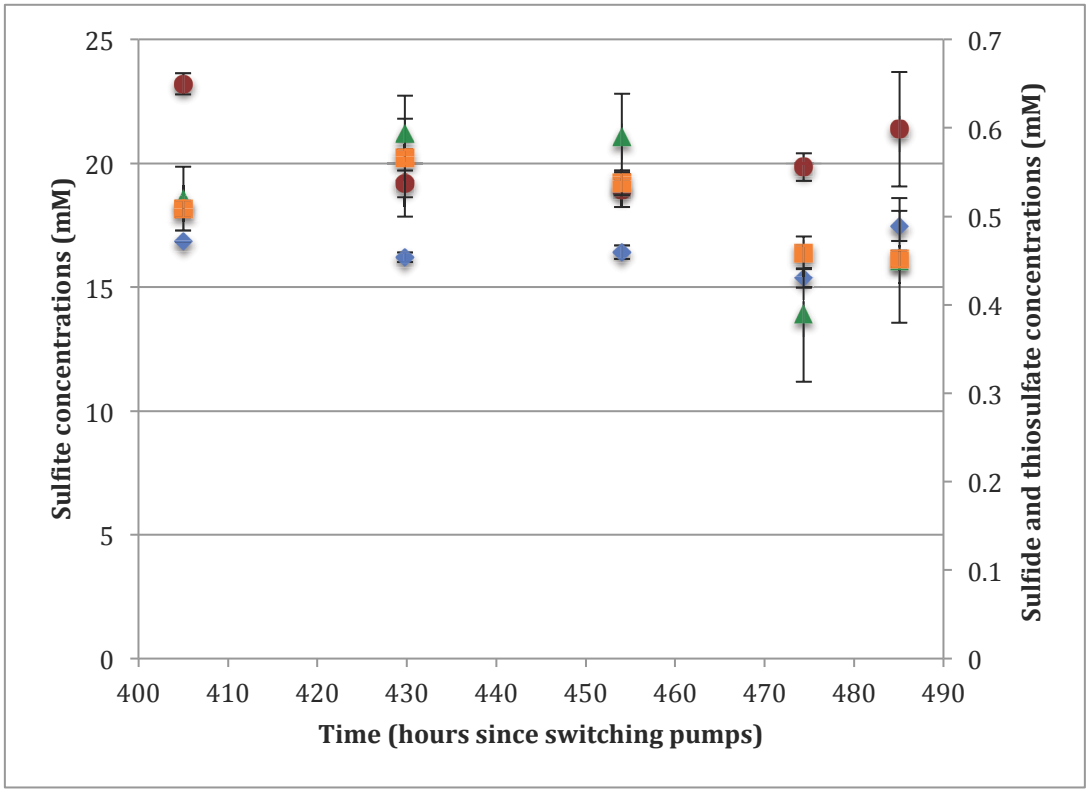

Figure 4: Sulfur budget in the reactor. Sulfite (blue diamonds), sulfide (green triangles) and thiosulfate (orange squares) concentrations for the reactor are shown. Sulfite concentrations for the 10L reserve batch media are shown (red circles) as a reference. Error bars correspond to 1 SD.

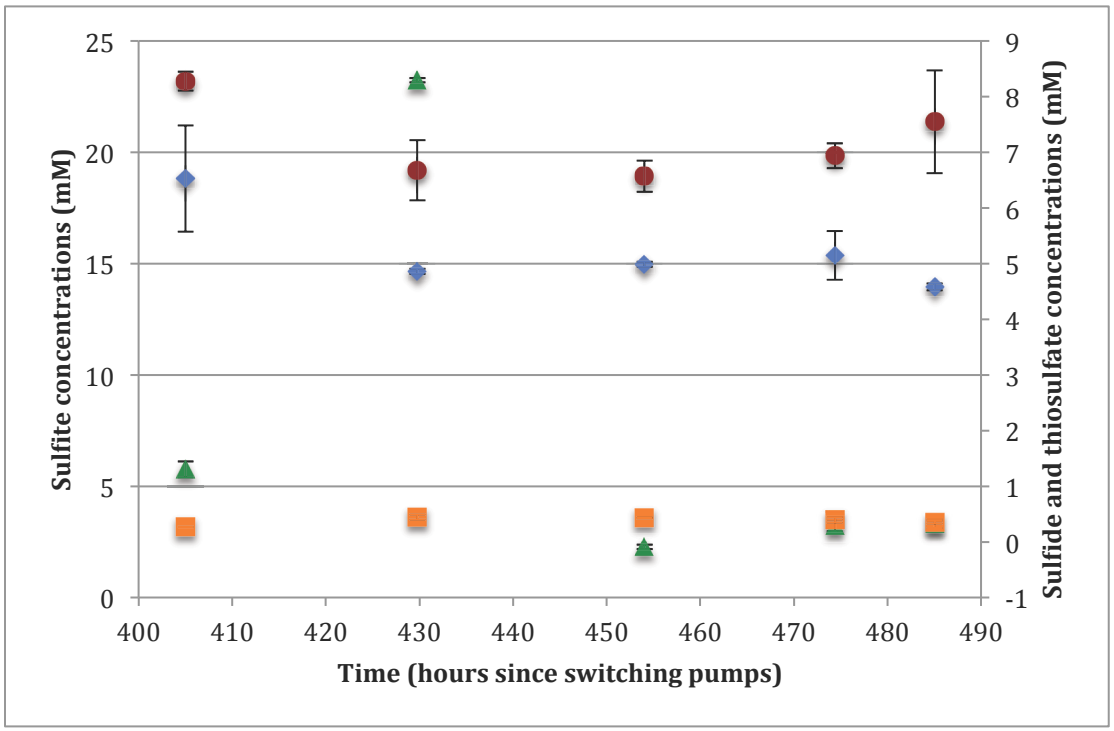

Figure 5: Sulfur budget in the liquid trap. Sulfite (blue diamonds), sulfide (green triangles) and thiosulfate (orange squares) concentrations for the reactor are shown. Sulfite concentrations for the 10L reserve batch media (red circles) are shown as a reference. Error bars correspond to 1 SD.

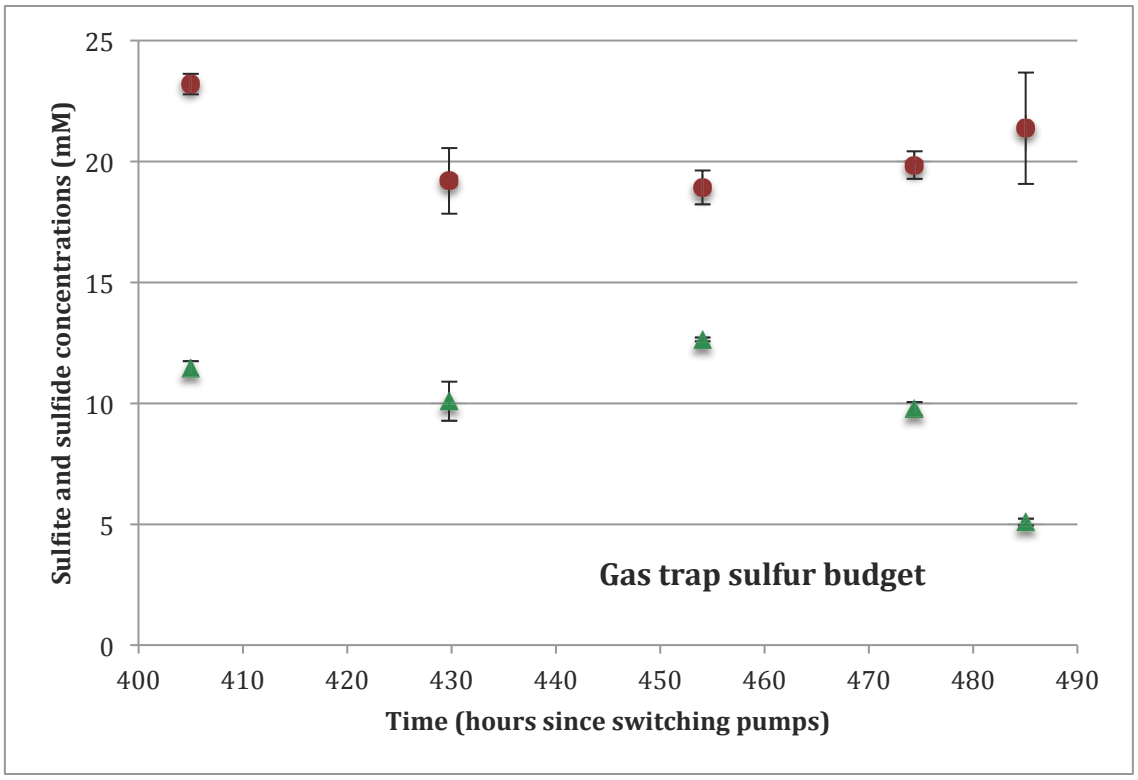

Figure 6: Sulfur budget in the gas trap. Sulfide (green triangles) concentrations for the gas trap are shown. Sulfite concentrations for the 10L reserve batch media (red circles) are shown as a reference. Error bars correspond to 1 SD.

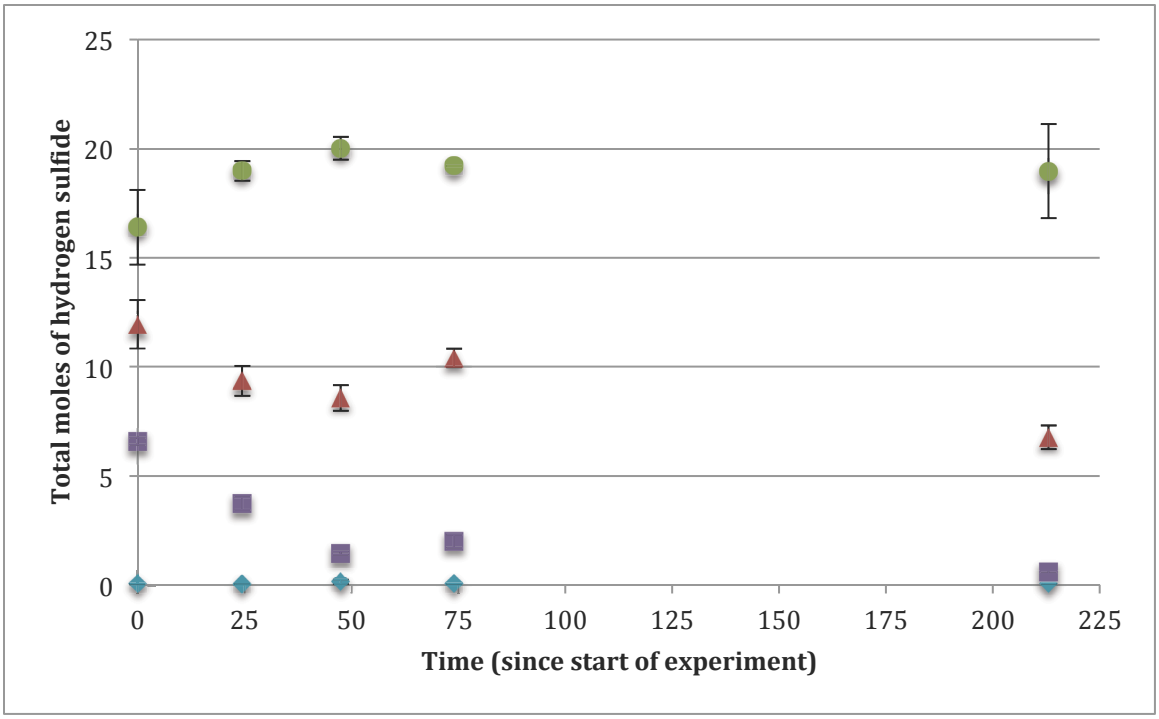

Figure 7: Concentration of hydrogen sulfide (mM) in solution through the course of the abiotic experiment for lines 1 (control line, blue diamonds), 2 (purple squares), 3 (red triangles) and 4 (green circles). Error bars shown correspond to 1 SD.

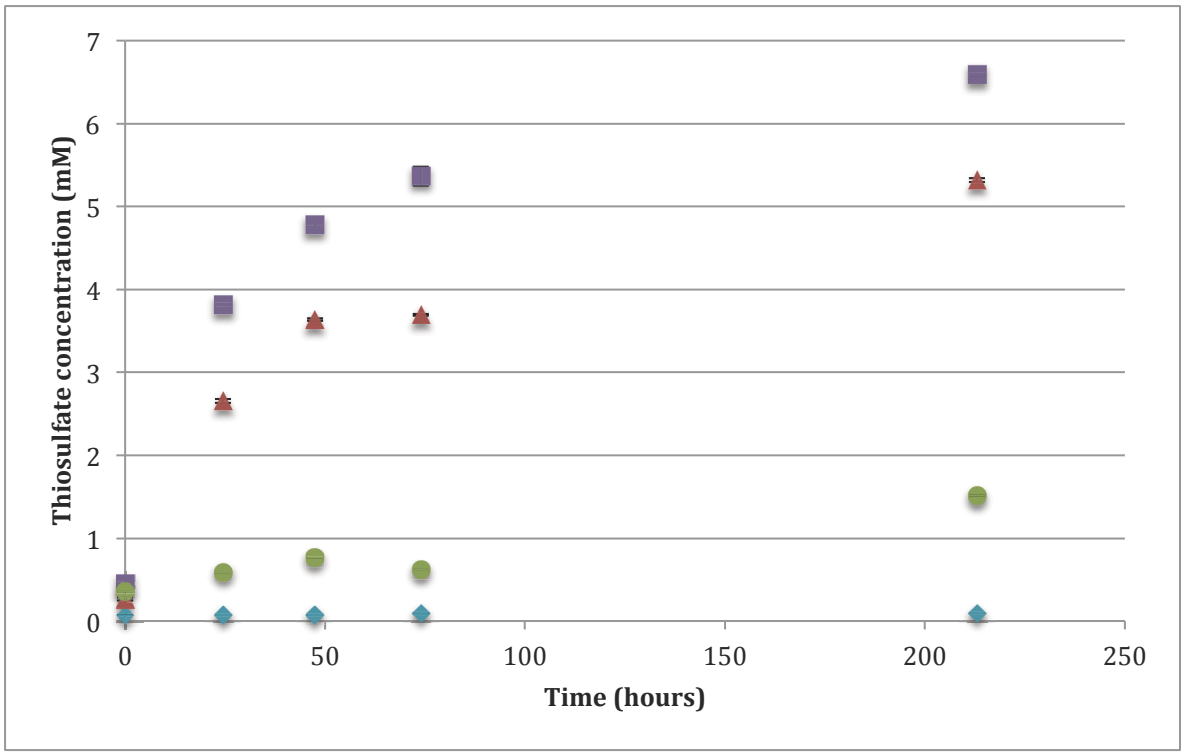

Figure 8: Concentration of thiosulfate (mM) in solution through the course of the experiment for lines 1 (control line, blue diamonds), 2 (purple squares), 3 (red triangles) and 4 (green circles). Error bars shown correspond to 1 SD.

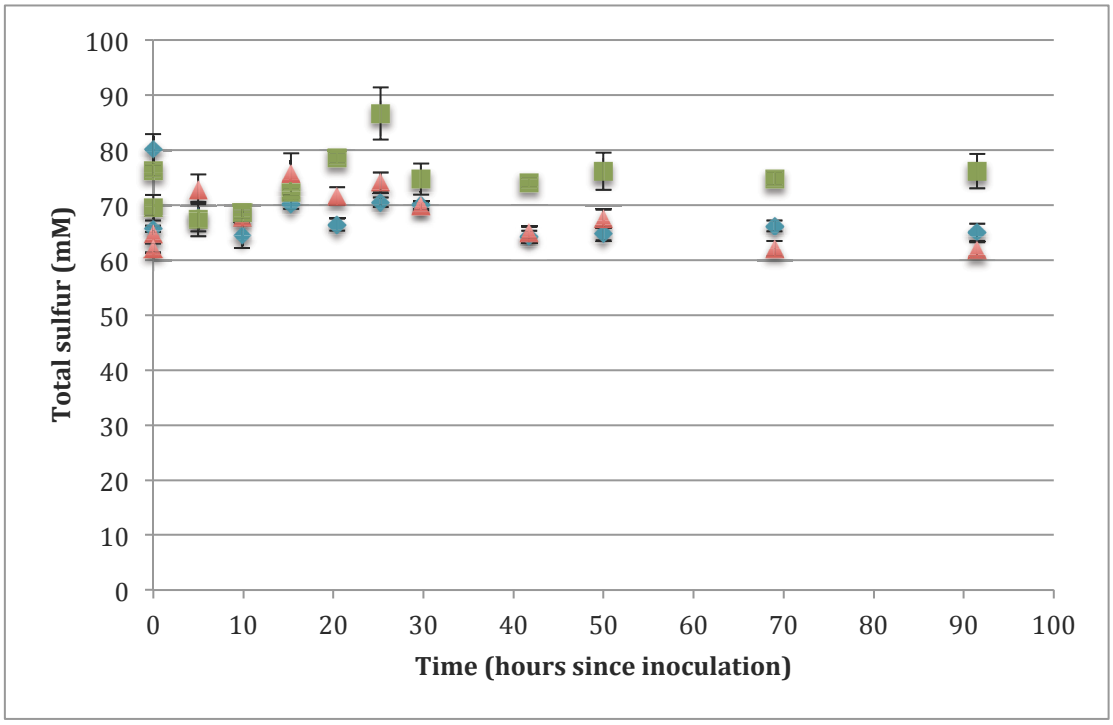

Figure 9: Total sulfur at each time point for each triplicate line (1: blue diamonds; 2: orange triangles; 3: green squares). Error bars represent 1 SD.

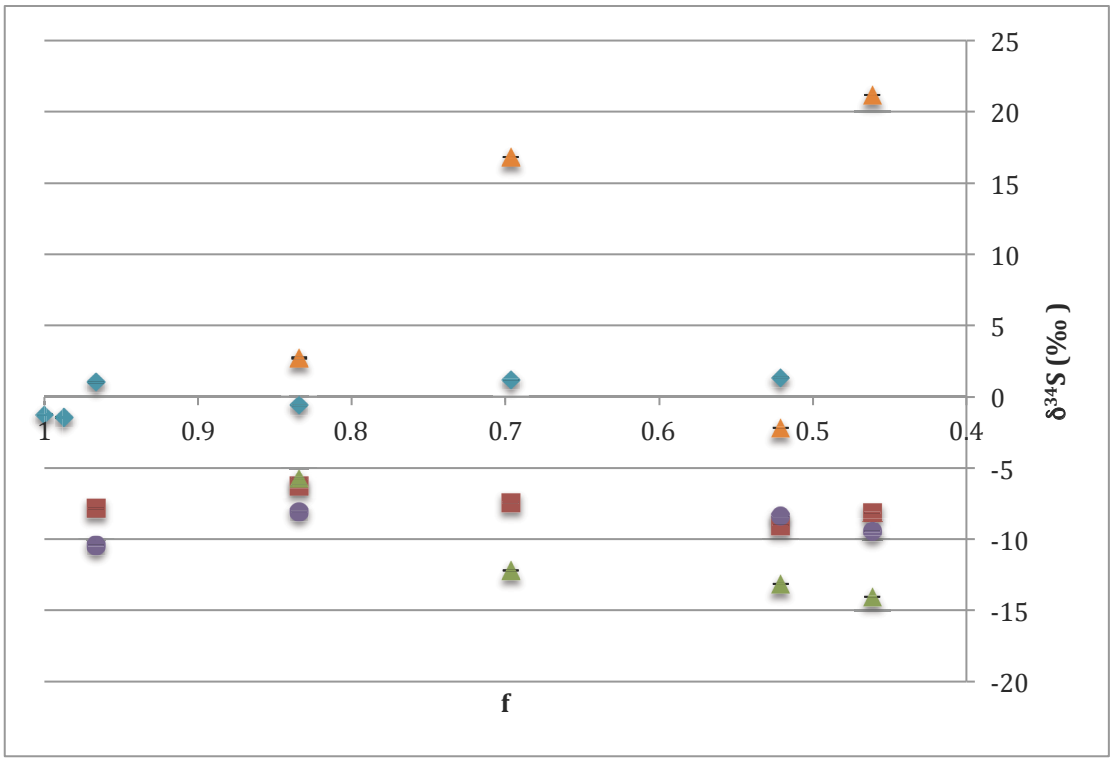

Figure 10: Evolution of the isotopic composition ($\delta^{34}S$, in ‰) of sulfite (blue diamonds), sulfide (red squares) and the sulfane (green triangles) and sulfonate groups (orange triangles) of thiosulfate and elemental sulfur (purple circles) in triplicate 1. Error bars correspond to 1 SD.

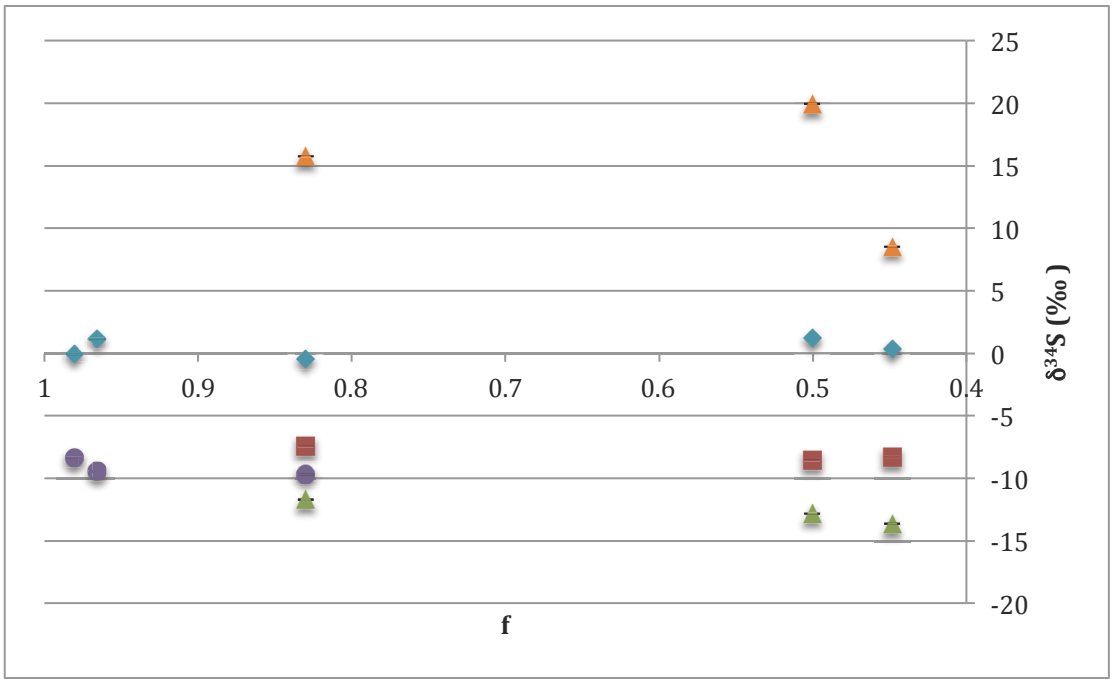

Figure 11: Evolution of the isotopic composition ($\delta^{34}S$, in ‰) of sulfite (blue diamonds), sulfide (red squares) and the sulfane (green triangles) and sulfonate groups (orange triangles) of thiosulfate and elemental sulfur (purple circles) in triplicate 2. Error bars correspond to 1 SD.

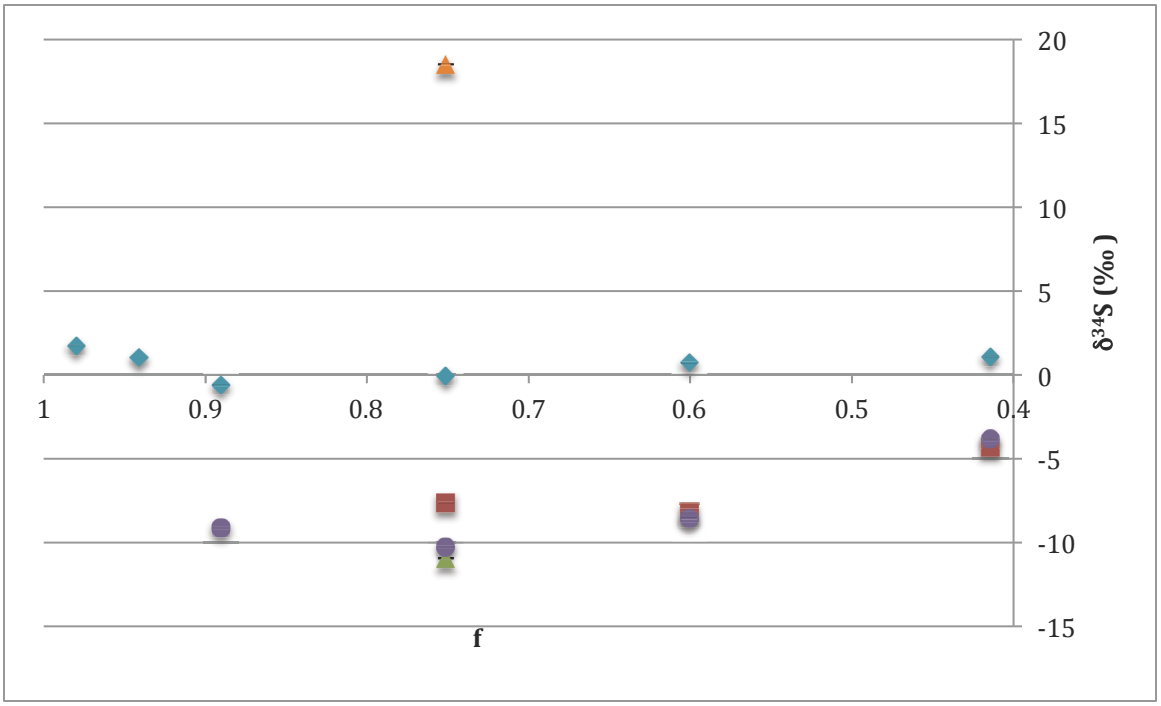

Figure 12: Evolution of the isotopic composition ($\delta^{34}S$, in ‰) of sulfite (blue diamonds), sulfide (red squares) and the sulfane (green triangles) and sulfonate groups (orange triangles) of thiosulfate and elemental sulfur (purple circles) in triplicate 3. Error bars correspond to 1 SD.

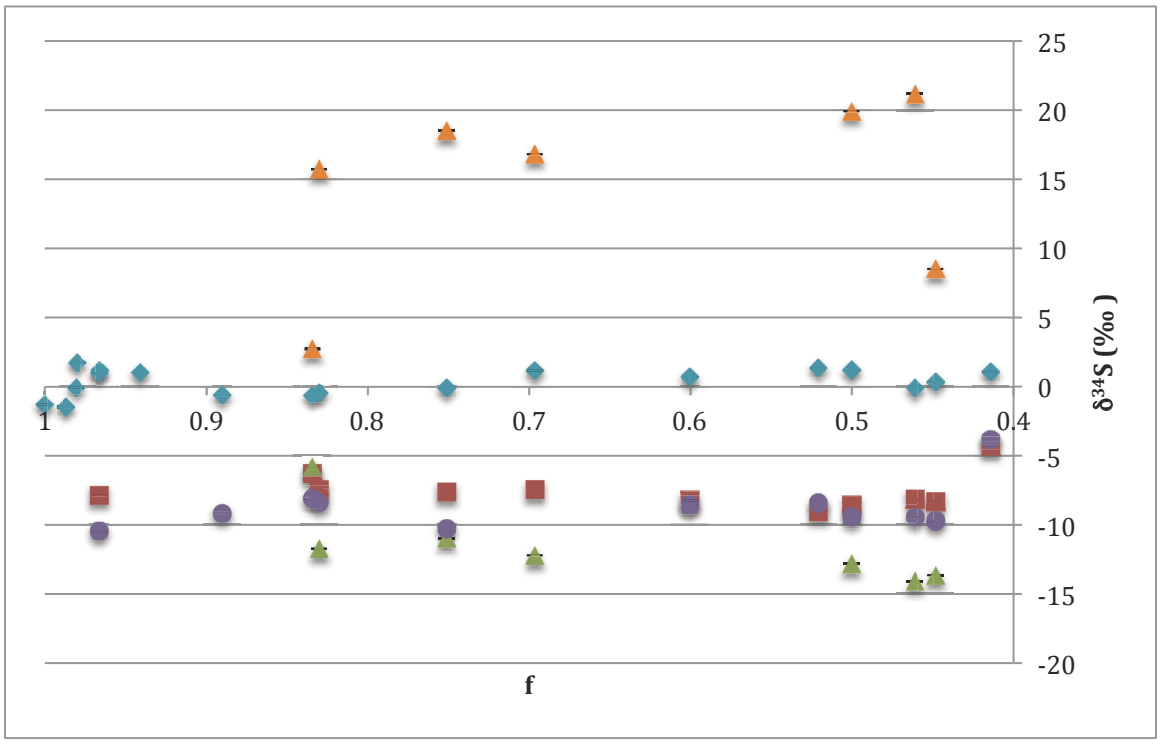

Figure 13: Evolution of the isotopic composition ($\delta^{34}S$, in ‰) of sulfite (blue diamonds), sulfide (red squares) and the sulfane (green triangles) and sulfonate groups (orange triangles) of thiosulfate and elemental sulfur (purple circles) of all triplicates. Error bars correspond to 1 SD.

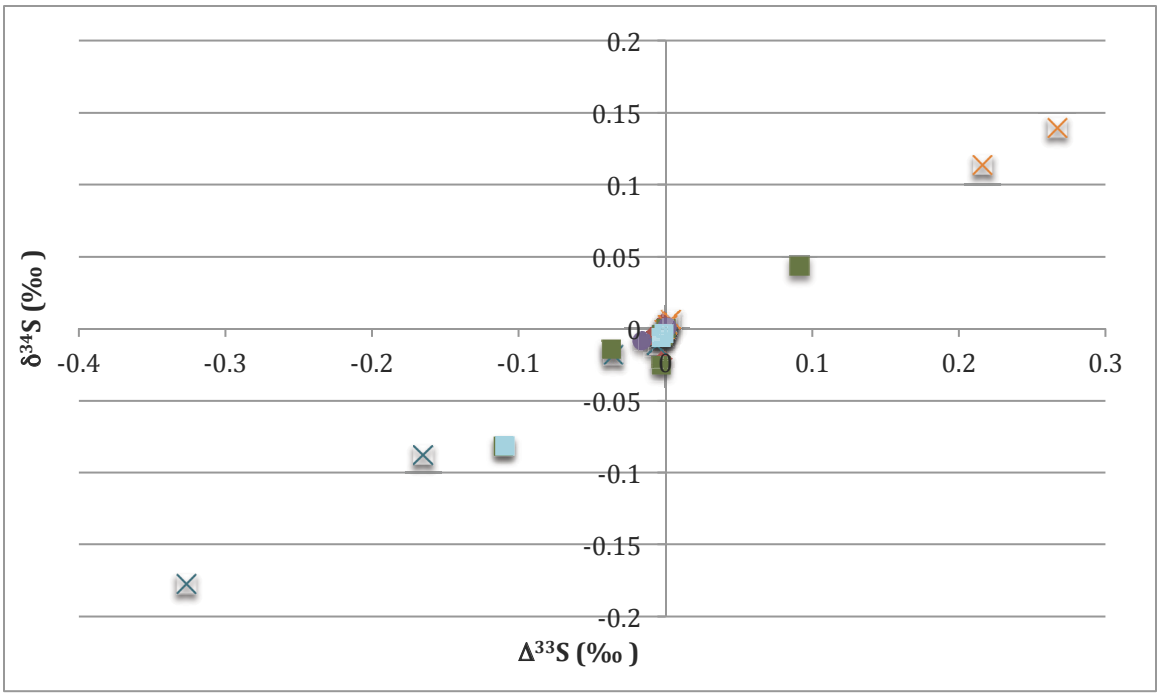

Figure 14: $\Delta^{33}S$ versus $\delta^{34}S$ (both in units of ‰), corrected for initial sulfite's isotopic composition and total moles corresponding to each phase, of initial sulfite (dark red diamond at the origin), sulfite (lighter red diamonds), sulfide (blue triangles), sulfane (orange crosses), sulfonate (blue crosses), elemental sulfur (purple circles) and the "mixing component" without included the elemental sulfur phase (green squares) and including it (light blue squares). Data shown corresponds to averages across all three triplicates.

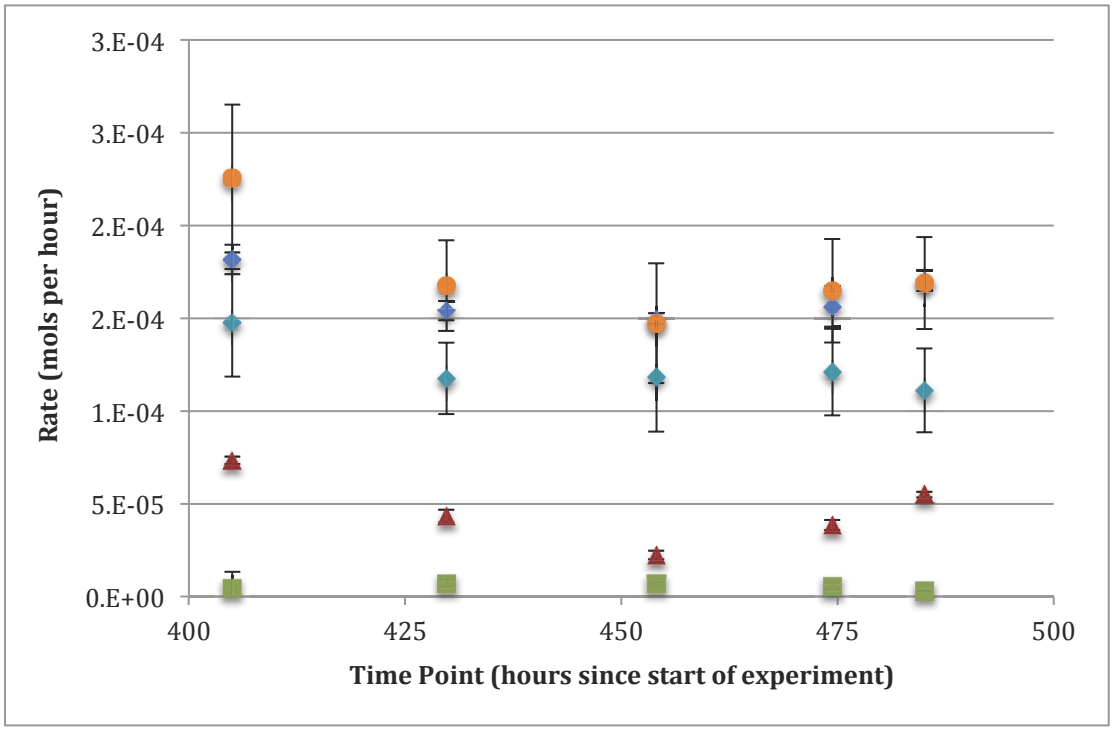

Figure 15: Rate (in moles per hour) of sulfite flowing in (blue diamonds) and out of the reactor (blue-green diamonds), sulfide (red triangles), thiosulfate (green squares) and total sulfur (orange circles) leaving the reactor. Error bars correspond to 1 SD after error propagation.

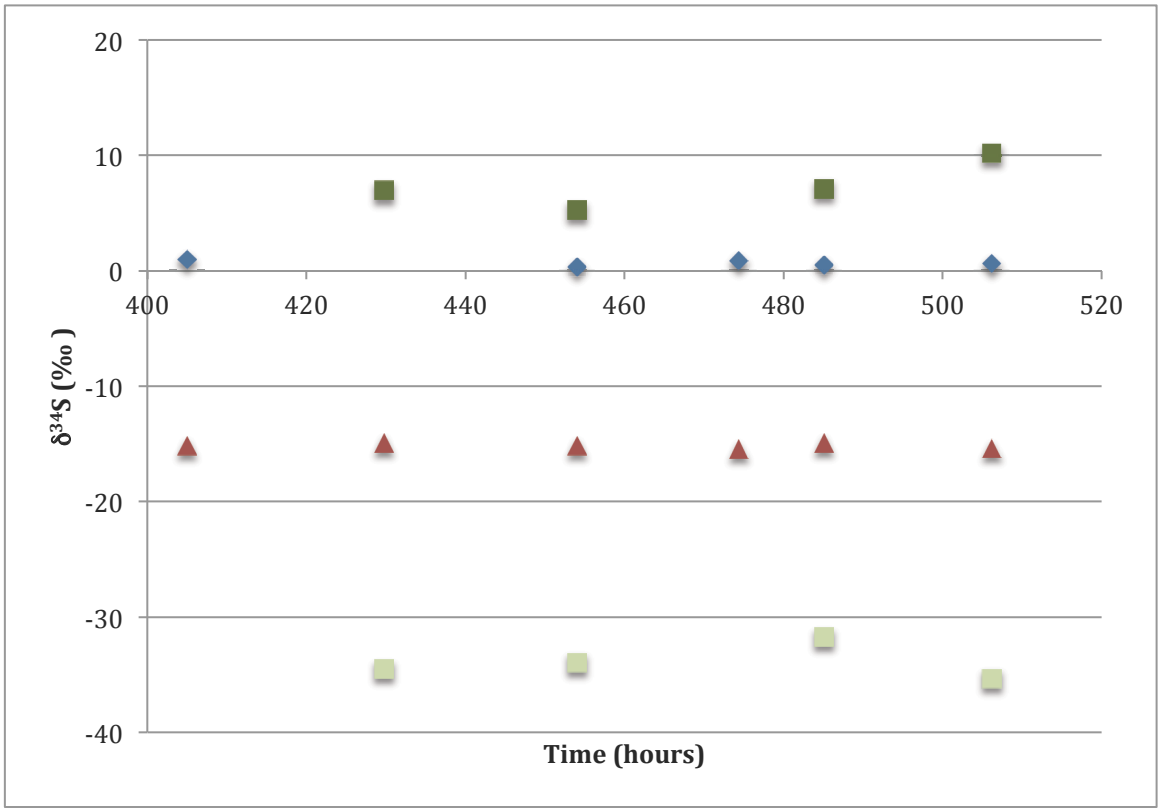

Figure 16: Isotopic composition (in $\delta^{34}S$, in units of ‰) of sulfite (blue diamonds), sulfide (red triangles), sulfonate (dark green squares) and sulfane (light green squares) during steady state

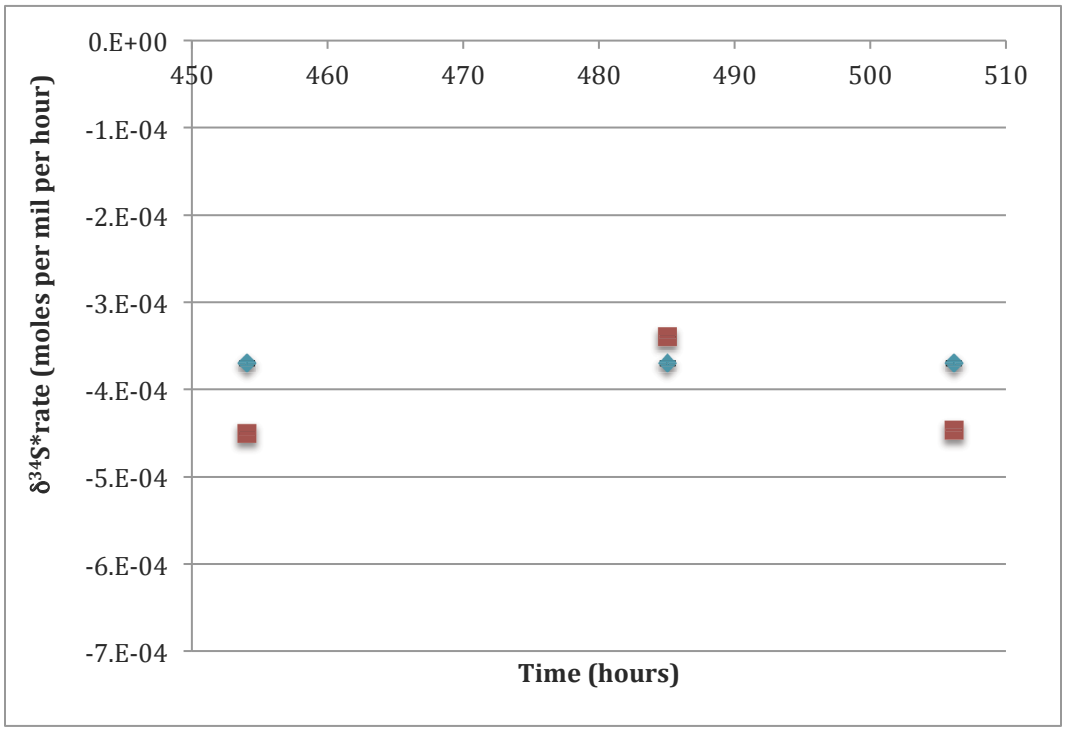

Figure 17: Isotopic composition of the total sulfur entering (blue diamonds) and leaving (red squares) the reactor at each sampling point during steady state. Error bars shown correspond to 1 SD.

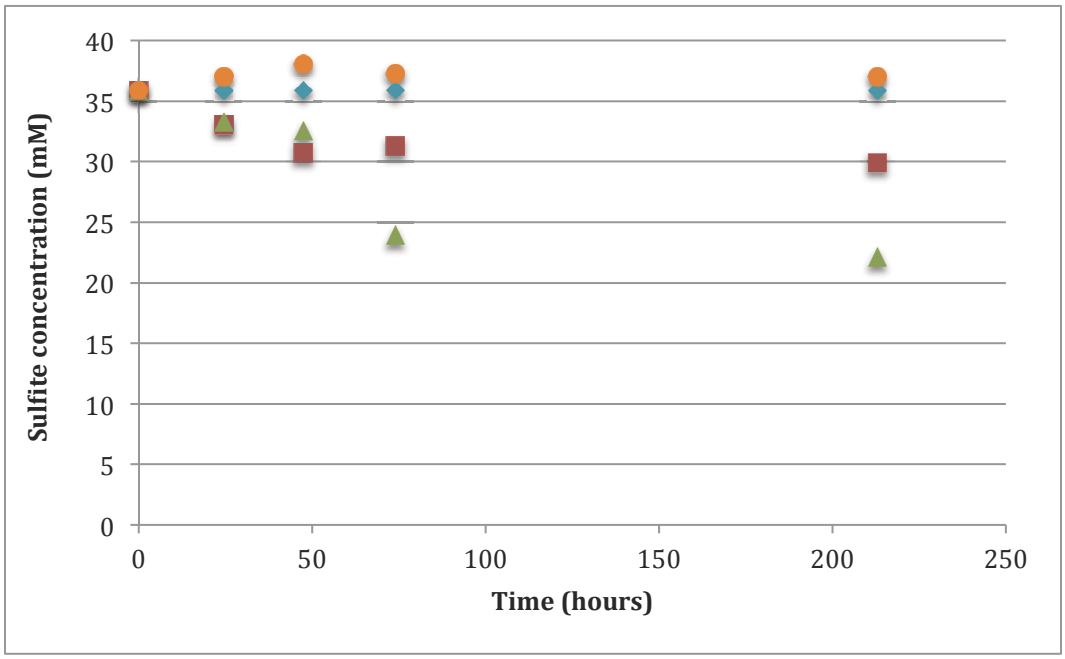

Figure 18: Sulfite levels deduced from sulfide and thiosulfate concentration data for line 1 (no initial sulfide, blue diamonds), 2 (6.59 mM initial sulfide, red squares), 3 (12 mM initial sulfide, green triangles) and 4 (18 mM initial sulfide, orange circles)

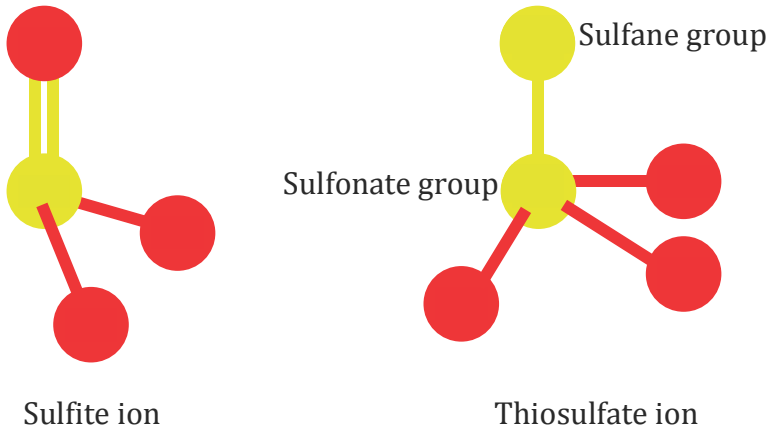

Figure 19: Molecular structure of the sulfite and the thiosulfate ions, the groups (sulfane and sulfonate) of thiosulfate are indicated as well; red balls are oxygen atoms, yellow ones correspond to sulfur atoms

Tables

	$\delta^{34}S$ (‰)			
Triplicate 1	SO_3	H_2S	Sulfane	Sulfonate
0	-1.272			
0	-1.451			
5	1.001	-7.837		
15.317	-0.621	-6.260	-5.747	2.729
20.417	1.181	-7.426	-12.192	16.837
41.750	-0.057	-8.138	-14.042	21.185
Triplicate 2				
0	-0.062			
5	1.158			
15.317	-0.464	-7.443	-11.712	15.732
25.250	1.222	-8.577	-12.819	19.922
29.750	0.342	-8.295	-13.631	8.521
Triplicate 3				
0	1.732			
5	1.022			
9.883	-0.604	-9.133		
15.317	-0.090	-7.628	-10.942	18.522
20.417	0.721	-8.228		
29.750	1.085	-4.301		

Table 1: Major isotope data ($\delta^{34}S$, in units of ‰) of the sulfite, sulfide, sulfane and sulfonate phases in the closed system experiment

	$\delta^{33}S$ (‰)			
Triplicate 1	SO_3	H_2S	Sulfane	Sulfonate
0	-0.612			
0	-0.707			
5	0.515	-4.053		
15.317	-0.268	-3.235	-2.974	1.423
20.417	0.636	-3.819	-6.271	8.645
41.750		-4.177	-7.193	10.878
Triplicate 2				
0	-0.013			
5				
15.317		-3.810	-6.015	8.097
25.250		-4.394	-6.550	10.241
29.750	0.194	-4.283	-6.991	4.401
Triplicate 3				
0	0.903			
5				
9.883	-0.266			
15.317		-3.891	-5.592	9.511
20.417	0.391	-4.242		
29.750	0.602	-2.181		

Table 2: Minor isotope data ($\delta^{33}S$, in units of ‰) of the sulfite, sulfide, sulfane and sulfonate phases in the closed system experiment

	$\delta^{36}S$ (‰)			
Triplicate 1	SO_3	H_2S	Sulfane	Sulfonate
0	-2.681			
0	-2.793			
5	1.945	-14.039		
15.317	-0.213	-11.295	-10.534	5.639
20.417	2.287	-13.885	-22.924	32.217
41.750		-15.555	-27.085	40.032
Triplicate 2				
0	-0.239			
5				
15.317		-14.258	-22.672	29.406
25.250		-16.520	-24.819	37.602
29.750	-0.275	-15.827	-25.268	15.896
Triplicate 3				
0	3.000			
5				
9.883	-1.427			
15.317		-15.057	-21.454	34.965
20.417	1.164	-15.784		
29.750	1.707	-7.056		

Table 3: Minor isotope data ($\delta^{36}S$, in units of ‰) of the sulfite, sulfide, sulfane and sulfonate phases in the closed system experiment

	CRS		
Triplicate 1	$\delta^{34}S$ (‰)	$\delta^{33}S$ (‰)	$\delta^{36}S$ (‰)
0			
0			
5	-10.434	-5.347	-20.240
15.317	-8.076	-4.132	-15.781
20.417			
41.750	-9.447	-4.824	-18.154
Triplicate 2			
0			
5			
15.317	-8.364	-4.274	-15.801
25.250	-9.419	-4.811	-18.133
29.750	-9.701	-4.978	-18.173
Triplicate 3			
0			
5			
9.883	-9.133	-4.703	-17.675
15.317	-10.278	-5.255	-19.906
20.417	-8.551	-4.372	-16.538
29.750	-3.820	-1.927	-5.963

Table 4: Major and minor isotope data ($\delta^{34}S$, $\delta^{33}S$, and $\delta^{36}S$, in units of ‰) of the CRS extract in the closed system experiment

Time	Phase	Sulfur species	$\delta^{34}S$ (‰)	$\delta^{33}S$ (‰)	$\delta^{36}S$ (‰)
405.010	Gas	H_2S	-15.178	-7.746	-27.982
	Liquid	SO_3	1.003	0.527	1.594
429.792	Gas	H_2S	-14.928	-7.677	-28.185
	Liquid	Sulfane	-34.531	-17.880	-63.990
	Liquid	Sulfonate	6.992	3.646	12.894
454.065	Gas	H_2S	-15.147	-7.808	-28.587
	Liquid	SO_3	0.338	0.192	0.521
	Liquid	Sulfane	-33.945	-17.570	-63.156
	Liquid	Sulfonate	5.252	2.736	8.719
474.391	Gas	H_2S	-15.450	-7.941	-29.209
	Liquid	SO_3	0.856	0.467	1.526
485.068	Gas	H_2S	-14.947	-7.680	-28.151
	Liquid	SO_3	0.477	0.264	0.749
	Liquid	Sulfane	-31.738	-16.458	-60.299
	Liquid	Sulfonate	7.058	3.648	12.164
506.162	Gas	H_2S	-15.354	-7.898	-28.835
	Liquid	SO_3	0.653	0.147	1.472
	Liquid	Sulfane	-35.341	-18.325	-67.166
	Liquid	Sulfonate	10.210	5.241	18.395

Table 5: Major and minor isotope data ($\delta^{34}S$, $\delta^{33}S$, and $\delta^{36}S$, in units of ‰) of the sulfite, sulfide, sulfane and sulfonate phases in the chemostat experiment

	1	2	3	Average
Sulfite consumed (moles)	1.563E-03	1.953E-03	1.626E-03	1.714E-03
Sulfide produced (moles)	4.827E-04	6.297E-04	5.746E-04	5.797E-04
Thiosulfate produced (moles)	5.939E-04	5.862E-04	7.077E-04	6.293E-04

Table 6: Total moles of consumed sulfite and produced sulfide and thiosulfate over the course of exponential phase in the batch experiment

	1	2	3	Average
Sulfite	1.00	1.00	1.00	1.00
Sulfide	0.31	0.32	0.35	0.34
Thiosulfate	0.38	0.30	0.44	0.37

Table 7: Stoichiometric coefficients of sulfite, sulfide and thiosulfate during sulfite reduction over the course of the exponential phase in the batch experiment

	1	2	3	Average
Sulfite consumption (moles/h)	-6.316E-05	-7.890E-05	-6.568E-05	-6.925E-05
Sulfide production (moles/h)	1.950E-05	2.544E-05	2.322E-05	2.342E-05
Thiosulfate production (moles/h)	2.399E-05	2.369E-05	2.860E-05	2.543E-05

Table 8: Rates of sulfite consumption, sulfide and thiosulfate production (in moles per hour) over the course of exponential phase in the batch experiment

	$\Delta^{33}S$ (‰)				
Triplicate 1	SO_3	H_2S	Sulfane	Sulfonate	Elemental sulfur
0	0.044				
0	0.041				
5	0.000	-0.010			0.040
15.317	0.052	-0.006	-0.010	0.019	0.035
20.417	0.028	0.012	0.027	0.009	
41.750		0.023	0.063	0.023	0.052
Triplicate 2					
0	0.019				
5					
15.317		0.031	0.034	0.026	0.042
25.250		0.032	0.072	0.030	0.050
29.750	0.018	-0.002	0.052	0.021	0.030
Triplicate 3					
0	0.012				
5					
9.883	0.045		-0.007	-0.004	0.011
15.317		0.044	0.058	0.015	0.051
20.417	0.020	0.003	0.003	0.001	0.041
29.750	0.044	0.037	0.018	0.008	0.042

Table 9: $\Delta^{33}S$ (in units of ‰) of the sulfite, sulfide, sulfane, sulfonate and thiosulfate phases across triplicates over the course of the exponential phase of the closed system experiment

Triplicate 1	Moles of "elemental sulfur"
0	
0	
5	
15.317	3.037E-04
20.417	
41.750	9.131E-04
Triplicate 2	
0	
5	
15.317	-2.046E-04
25.250	-1.712E-06
29.750	-8.153E-04
Triplicate 3	
0	
5	
9.883	
15.317	-4.854E-04
20.417	
29.750	

Table 10: Moles of the "elemental sulfur" phase across triplicates over the course of the exponential phase of the batch experiment

Rate of sulfite consumption (moles/h)	4.159E-05
Rate of sulfide production (moles/h)	3.829E-05
Rate of thiosulfate production (moles/h)	3.320E-06

Table 11: Rates of sulfite consumption and sulfide and thiosulfate production (in moles per hour) in the chemostat experiment while steady state was maintained

Sulfite	1.00
Sulfide	0.92
Thiosulfate	0.08

Table 12: Stoichiometric coefficients of sulfite, sulfide and thiosulfate during the reduction of sulfite while steady state was maintained in the chemostat experiment

	α^{34}		
Time	SO_3-H_2S	SO_3-S_2O_3	S_2O_3-H_2S
405.010	0.9838		
429.792			
454.065	0.9845	0.9853	0.9992
474.391	0.9837		
485.068	0.9846	0.9872	0.9974
506.162	0.9840	0.9868	0.9972

Table 13: α^{34} between sulfite and sulfide, between sulfite and thiosulfate and between thiosulfate and sulfide while steady state was maintained in the chemostat experiment

	α^{33}		
Time	SO_3-H_2S	SO_3-S_2O_3	S_2O_3-H_2S
405.010	0.9917		
429.792			
454.065	0.9920	0.9924	0.9996
474.391	0.9916		
485.068	0.9921	0.9933	0.9987
506.162	0.9920	0.9933	0.9986

Table 14: α^{33} between sulfite and sulfide, between sulfite and thiosulfate and between thiosulfate and sulfide while steady state was maintained in the chemostat experiment

Line	Sulfide consumption (moles/h)	Thiosulfate production (moles/h)
1	3.00E-10	1.00E-09
2	-2.00E-07	2.00E-07
3	-2.00E-07	2.00E-07
4	2.00E-08	5.00E-08

Table 15: Rates of sulfide consumption and thiosulfate production (in units of mM per hour) in each abiotic experiment

Acronym	Symbol	Unit	Full name
Ma			Millions of years
SRB			Sulfate Reducing Bacteria
DSR			Dissimilatory Sulfate Reduction
Ga			Billions of years
	‰		per mil
APS			Adenosine 5'-PhosphoSulfate
ATP			Adenosine TriPhosphate
Sat			ATP sulfurylase
AMP			Adenosine MonoPhosphate
QmoABC			Quinone-interacting Membrane-bound Oxidoreductase ABC complex
qmoA			Quinone-interacting Membrane-bound Oxidoreductase A
qmoB			Quinone-interacting Membrane-bound Oxidoreductase B
qmoC			Quinone-interacting Membrane-bound Oxidoreductase C
AprABC			APS Reductase ABC
	SO_3^{2-}		Sulfite
	$S_2O_3^{2-}$		Thiosulfate
	$S_3O_6^{3-}$		Trithionate
	S^{2-}		Sulfide
DsrAB			Dissimilatory Sulfite Reductase AB
DsrC			Dissimilatory Sulfite Reductase C
	%		per cent
	R_X		Heavy to light isotope ratio in species X
	OD_{600}		Optical density at 600 nm
psi			Pound per Square Inch
AVS			Acid Volatile Sulfur
CRS			Chromium Reducible Sulfur
f			Fraction of reactant remaining
	υ_B	moles per hour	Rate of formation or consumption of sulfite, sulfide or thiosulfate due to biotic effects
	υ_{abio}	moles per hour	Rate of formation or consumption of sulfite, sulfide or thiosulfate due to abiotic effects
	x	moles per hour	Rate of formation or consumption of thiosulfate due to biotic effects

Table 16: List of symbols, acronyms and corresponding unit and name used, in order of appearance

References

Akagi, J. M. (1995). "Respiratory sulfate reduction," in *Sulfate-Reducing Bacteria,* ed. L. L. Barton (New York: Plenum Press), 89–111

Akagi, J. M., Campbell, L. L. (1962) Studies on thermophilic sulfate-reducing bacteria. III. Adenosine triphosphate-sulfurylase of Clostridium nigrificans and Desulfovibrio desulfuricans, *J. Bacteriol*, vol. 84, no. 6, 1194-1201

Akagi, J. M., Campbell, L. L. (1963) Inorganic pyrophosphatase of Desulfovibrio desulfuricans, *J. Bacteriol*, vol. 86, no. 3, 563-568

Aketagawa, J., Kobayashi, K., Ishimoto, M. (1985) Purification and properties of thiosulfate reductase from Desulfovibrio vulgaris, Miyazaki F, *The Journal of Biochemistry*, vol. 97, no. 4, 1025-1032

Berner RA, Canfield DE (1989) A new model for atmospheric oxygen over Phanerozoic time. *Am J Sci*, vol. 289, no. 4, 333–361

Berner, R.A., (1982) Burial of organic-carbon and pyrite sulfur in the modern ocean, its geochemical and environmental significance. *American Journal of Science,* vol. 282, no. 4, 451–473.

Bolliger C., Schroth M. H., Bernasconi S. M., Kleikemper J., and Zeyer, J. (2001) Sulfur isotope fractionation during microbial sulfate re- duction by toluene-degrading bacteria. *Geochim. Cosmochim. Acta* vol. 65**,** 3289–3298.

Broco, M., Rousset, M., Olveira, S. Rodrigues-Pousada, C. (2005) Deletion of flavoredoxin gene in Desulfovibrio gigas reveals its participation in thiosulfate reduction, *FEBS Letters*, vol. 579, 4803-4807

Brunner B. and Bernasconi S. M. (2005) A revised isotope fractionation model for dissimilatory sulfate reduction in sulfate reducing bacteria. *Geochim. Cosmochim. Acta* vol*.* 69, no. 20, 4759–4771.

Canfield D. E. and Thamdrup B. (1994) The production of ^{34}S-depleted sulfide during bacterial disproportionation of elemental sulfur. *Science* vol. 266**,** 1973–1975.

Canfield DE, Habicht KS, Thamdrup B (2000) The Archean sulfur cycle and the early history of atmospheric oxygen. *Science* vol. 288, 658-661

Canfield DE (2001) Isotope fractionation by natural populations of sulfate-reducing bacteria. *Geochim Cosmochim Acta* vol. 65, 1117-1124

Canfield, D. E. (2001) Biogeochemistry of sulfur isotopes, *Reviews in Mineralogy and Geochemistry*, vol. 43, no. 1, 607-636.

Canfield, D.E., 2004. The evolution of the Earth surface sulfur reservoir. *American Journal of Science* vol. 304, no. 10, 839–861.

Canfield DE, Olesen CA, Cox RP (2006) Temperature and its control of isotope fractionation by a sulfate-reducing bacterium. *Geochim Cosmochim Acta* vol. 70, no. 3, 548–561.

Castro, H. F., Williams, N. H., Ogram, A. (2000) Phylogeny of sulfate-reducing bacteria, *FEMS Microbiol. Ecol.*, vol. 31, 1-9

Chambers, L. A., Trudinger, P. A., Smith, J. W., Burns, M. S. (1975) Fractionation of sulfur isotopes by continuous cultures of Desulfovibrio desulfuricans, *Can. J. Microbiol.*, vol. 21, 1602-1607

Chambers L. A., Trudinger P. A., Smith J. W. and Burns M. S. (1976) Possible boundary-condition in bacterial sulfur isotope fractionation. *Geochim. Cosmochim. Acta* vol. 40, 1191–1194.

Chambers L. A., Trudinger P. A. (1979) Thiosulfate formation and associated isotope effects during sulfite reduction by Clostridium pasteurianum. *Can. J. Microbiol.* vol. 25, 719-721

Claypool G. E. (2004) Ventilation of marine sediments indicated by depth profiles of pore water sulfate and $\delta^{34}S$. In *Geochemical Investigations in Earth and Space Science: A Tribute to Isaac R. Kaplan,* Special Publications 9, (ed. R. J. Hill et al.) 59 – 65, The Geochemical Society.

Craig H., Horibe Y. and Sowers T. (1988) Gravitational separation of gases and isotopes in polar ice caps. *Science* vol. 242, 1675–1678.

Detmers, J., Bruchert, V., Habicht, K. S., Kuever, J. (2001) Diversity of sulfur isotope fractionations by sulfate-reducing prokaryotes, *Appl. Environ. Microbiol.,* vol. 67, 888-894

Drake, H. L., Akagi, J. M. (1977) Bisulfite reductase of Desulfovibrio vulgaris: explanation for product formation, *Journal of Bacteriology*, vol. 132, no. 1, 139-143

Farquhar, J., Bao, H. M., and Thiemens, M., 2000, Atmospheric influence of Earth's earliest sulfur cycle: *Science*, vol. 289, 756 –758

Farquhar, J., Savarino, J., Airieau, S., Thiemens, M.H., 2001. Observation of wavelength- sensitive mass-independent sulfur isotope effects during SO2 photolysis: implications for the early atmosphere. *Journal of Geophysical Research, Planets* vol. 106, (E12), 32829–32839

Farquhar J., Johnston D. T., Wing B. A., Habicht K. S., Canfield D. E., Airieau S., and Thiemens M. H. (2003) Multiple sulphur isotopic interpretations of biosynthetic pathways: implications for biological signatures in the sulphur isotope record. *Geobiology* vol. 1**,** 27–36.

Farquhar J. and Wing B. A. (2003) Multiple sulfur isotopes and the evolution of the atmosphere. *Earth Planet. Sci. Lett*. vol. 213, 1–13.

Farquhar J. and Wing B. A. (2005) The terrestrial record of stable sulphur isotopes: a review of the implications for the evolution of Earth's sulphur cycle. In *Mineral Deposits and Earth Evolution*. Geological Society, London, 167–177 (Special publication).

Farquhar, J., Johnston, D.T., Wing, B.A. (2007) Implications of conservation of mass effects on mass-dependent isotope fractionations: influence of network structure on sulfur isotope phase space of dissimilatory sulfate reduction. *Geochimica Et Cosmochimica Acta* vol. 71, no. 24, 5862–5875.

Findley, J. E., Akagi, J. M. (1969) Evidence for thiosulfate formation during sulfite reduction by Desulfovibrio vulgaris, *Biochemical and Biophysical Research Communications*, vol. 36, no. 2, 266-271

Findley, J. E., Akagi, J. M. (1970) Role of thiosulfate in bisulfite reduction as catalyzed by Desulfovibrio vulgaris, *J. Bacteriol.*, vol. 103, no. 3, 741-744

Fitz, R. B., Cypionka, H. (1990) Formation of thiosulfate and trithionate during sulfite reduction by washed cells of Desulfovibrio desulfuricans, *Arch. Microbiol*, vol. 154, 400-406

Fitz, R. M., Cypionka, H. (1991) Generation of a proton gradient in Desulfovibrio vulgaris*. Arch. Microbiol*, vol. 155, 444–448

Frederikson, T.M., Finster, K., (2003) Sulfite-oxido-reductase is involved in the oxidation of sulfite in Desulfocapsa sulfoexigens during disproportionation of thiosulfate and elemental sulfur. *Biodegradation* vol. 14, no. 3, 189–198.

Fry B., Ruf W., Gest H., and Hayes J. M. (1988) Sulfur isotope effects associated with oxidation of sulfide by O2 in aqueous solution. *Chem. Geol.* vol. 73**,** 205–210.

Garrels Rm, Lerman A (1981) Phanerozoic cycles of sedimentary carbon and sulfur. *Proceedings of the National Academy of Sciences of the United States of America - Physical Sciences,* vol. 78**,** 4652-4656.

Habicht K. S. and Canfield D. E. (2001) Isotope fractionation by sulfate-reducing natural populations and the isotopic composition of sulfide in marine sediments. *Geology* vol. 29**,** 555–558.

Habicht, KS, Gade, M, Thamdrup, B, Berg, P, Canfield, DE (2006) Calibration of sulfate levels in the Archean ocean, *Science,* vol. 298, 2372-2374

Harrison A. G. and Thode H. G. (1958) Mechanism of the bacterial reduction of sulphate from isotope fractionation studies. *Trans. Faraday Soc.* vol. 54**,** 84–92.

Haschke, R. H., Campbell, L. L. (1971) Purification and properties of a hydrogenase from Desulfovibrio vulgaris, *Journal of Bacteriology*, vol. 105, no. 1, 249-258

Hatchikian, E. C. (1975) Purification and properties of thiosulfate reductase form Desulfovibrio gigas, *Archives of Microbiology*, vol. 105, no. 1, 249-256

Heidelberg JF, Seshadri R, Haveman SA, Hemme CL, Paulsen IT, Kolonay JF, Eisen JA, Ward N, Methe B, Brinkac LM, Daugherty SC, Deboy RT, Dodson RJ, Durkin AS, Madupu R, Nelson WC, Sullivan SA, Fouts D, Haft DH, Selengut J, Peterson JD, Davidsen TM, Zafar N, Zhou LW, Radune D, Dimitrov G, Hance M, Tran K, Khouri H, Gill J, Utterback TR, Feldblyum TV, Wall JD, Voordouw G, Fraser CM (2004) The genome sequence of the anaerobic, sulfate-reducing bacterium Desulfovibrio vulgaris Hildenborough. *Nat Biotechnol,* vol. 22, 554–559

Hulston J. R. and Thode H. G. (1965) Cosmic ray produced ^{36}S and ^{33}S in metallic phase of iron meteorites. J. Geophys. Res. vol. 70, 4435–4442.

Ishimoto, M., Koyama, J., Nagai, Y. (1955) Biochemical studies on suflate-reducing bacteria. IV. Reduction of thiosulfate by cell-free extracts, *J. Biochem.*, vol. 42, no. 1, 41-45

Ishimoto, M., Fujimoto, D. (1961) Biochemical studies on sulfate-reducing bacteria. X. Adenosine-5'-phosphosulfate reductase, *The Journal of Biochemistry*, vol. 50, no. 4, 299-304

Johnston D. T., Farquhar J., Wing B. A., Kaufman A., Canfield D. E. and Habicht K. S. (2005) Multiple sulfur isotope fractio- nations in biological systems: a case study with sulfate reducers and sulfur disproportionators. *Am. J. Sci*. vol. 305, (6–8), 645–660.

Johnston, D. T., Farquhar, J., Canfield, D. E. (2007) Sulfur isotope insights into microbial sulfate reduction: when microbes meet models, *Geochimica et Cosmochimica Acta* vol. 71, 3929–3947

Johnston, D.T., Wolfe-Simon, F., Pearson, A., Knoll, A.H., (2009) Anoxygenic photosyn- thesis modulated Proterozoic oxygen and sustained Earth's middle age. *Proceedings of the National Academy of Sciences of the United States of America* vol. 106, no. 40, 16925–16929.

Jorgensen, B.B., 1990. A thiosulfate shunt in the sulfur cycle of marine-sediments. *Science* vol. 249, no. 4965, 152–154.

Kaplan I. R. and Rittenberg S. C. (1964) Microbial fractionation of sulphur isotopes. *J. Gen. Micorbiol.* **34,** 195–212

Kemp A. L. W. and Thode H. G. (1968) The mechanism of bacterial reduction of sulphate and sulphite from isotope fractionation stud- ies. *Geochim. Cosmochim. Acta* **32,** 71–91.

Kobayashi, K., Tachibana, S., Ishimoto, M. (1969) Intermediary formation of trithionate in sulfite reduction by a sulfate-reducing bacterium, *The Journal of Biochemistry*, vol. 65, no. 1, pp. 155-157

Kobayashi, K., Takahash, E., Ishimoto, M., (1972). Biochemical studies on sulfate-reducing bacteria .11. Purification and some properties of sulfite reductase, desulfoviridin. *Journal of Biochemistry* 72 (4), 879.

Kobayashi, K., Seki, Y., Ishimoto, M., (1974) Biochemical studies on sulfate reducing bacteria. 13. Sulfite reductase from Desulfovibrio vulgaris—mechanism of trithio-nate, thiosulfate, and sulfide formation and enzymatic properties. *Journal of Biochemistry* 75 (3), 519–529.

Lee, J. P., Peck, H. D. (1971) Purification of the enzyme reducing bisulfite to trithionate from Desufovibrio gigas and its identification as desulfoviridin, *Biochemical and Biophysical Research Communications*, vol. 45, no. 3, pp. 583-589

Lupton, F. S., Conrad, R., Zeikus, J. G. (1984) Physiological-function of hydrogen metabolism during growth of sulfidogenic bacteria on organic substrates. *J Bacteriol*, vol. 159, pp. 843–849

Matias, P. M., Pereira, I. A., Soares, C. M., Carrondo, M. A. (2005) Sulphate respiration from hydrogen in Desulfovibrio bacteria: a structural biology overview. *Prog Biophys Mol Biol*, vol. 89, pp. 292–329

Miller M. F. (2002) Isotopic fractionation and the quantification of ^{170} anomalies in the oxygen three-isotope system: an appraisal and geochemical significance. *Geochim. Cosmochim. Acta* 66, 1881–1889.

Mook W. G. (2000) Environmental isotopes in the hydrological cycle principles and applications. V I: Introduction—Theory, Methods, Review, 1: Paris, UNESCO/IAEA.

Neretin L. N., Böttcher M. E., and Grinenko V. A. (2003) Sulfur isotope geochemistry of the Black Sea water column. *Chem. Geol.* **200,** 59–69.

O'Leary M. H. (1977) Studies of enzyme reaction mechanisms by means of heavy-atom isotope effects. In *Isotope Effects on Enzyme- Catalyzed Reactions* (eds. W. W. Cleland, M. H. O'Leary, and D. B. Northrop), pp. 233–251. University Park Press.

Odom, J. M., Peck, H. D. (1981) Hydrogen cycling as a general mechanism for energy coupling in the sulfate-reducing bacteria, Desulfovibrio sp., *FEMS Microbiol. Lett.,* vol. 12pp. 47-50

Ohmoto H., Kaiser C. J., and Geer K. A. (1990) Systematics of sulphur isotopes in recent marine sediments and ancient sediment-hosted basemetal deposits. In *Stable Isotopes and Fluid Processes in Mineralization.* Vol. 23 (ed. H. K. Herbert and S. E. Ho), pp. 70–120, Geology Department & University Extension, The Uni- versity of Western Australia.

Oliveira, T. F., Vonrhein, C., Matias, P. M., Venceslau, S. S., Pereira, I. A., and Archer, M. (2008). The crystal structure of *Desulfovibrio vulgaris* dissimilatory sulfite reductase bound to DsrC provides novel insights into the mechanism of sulfate respiration. *J. Biol. Chem.* 283, 34141–34149.

Parey, K., Warkentin, E., Kroneck, P. M. H., Ermler, U. (2010) Reaction cycle of the dissimilatory sulfite reductase from Archeoglobus fulgidus*, Biochemistry*, vol. 49, pp. 8912-8921

Pavlov, A.A., Kasting, J.F., 2002. Mass-independent fractionation of sulfur isotopes in Archean sediments: Strong evidence for an anoxic Archean atmosphere. *Astrobiology* 2 (1), 27–41.

Peck, H. D. (1959) The ATP-dependent reduction of sulfate with hydrogen in extracts of Desulfovibrio desulfuricans, *Proc. Natl. Acad. Sci. USA*, vol. 45, pp. 701-708

Peck, H. D. (1960) Evidence for oxidative phosphorylation during the reduction of sulfate with hydrogen by Desulfovibrio desulfuricans, *J. Biol. Chem.*, vol. 235, pp. 2734-2738

Peck, H. D. (1961) Evidence for reversibility of reaction catalyzed by adenosine 5'-phosphosulfate reductase, *Biochim. Biophys. Acta*, vol. 49, pp. 621-624

Peck H (1962) Comparative metabolism of inorganic sulfur compounds in microorganisms. *Bacteriological Reviews* 26, 67–94.

Peck, H. D., Legall, J. (1982) Biochemistry of dissimilatory sulfate reduction, *Phil. Trans. R. Soc. Lond.*, vol. 298, pp. 443-466

Pereira, I. A. C., Haveman, S. A., and Voordouw, G. (2007). "Biochemical, genetic and genomic characteriza- tion of anaerobic electron trans- port pathways in sulphate-reducing delta-proteobacteria," in *Sulphate- Reducing Bacteria: Environmental and Engineered Systems,* eds L. L. Barton and W. A. Allan Hamilton (Cambridge: Cambridge University Press), 215–240.

Pereira, I. A. C. (2008) Respiratory membrane complexes of Desulfovibrio, *Microbial Sulfur Metabolismi,* chap. 3, pp. 24-35

Pereira, I. A. C., Ramos, A. R., Grein, F., Coimbra Marques, M., Marques da Silva, S., Santos Venceslau, S. (2011) A comparative genomic analysis of energy metabolism in sulfate reducing bacteria and archaea, *Frontiers in Microbiology*, vol. 2, no. 69, pp. 1-22

Pires, R. H., Lourenco, A. I., Morais, F., Teixeira, M., Xavier, A. V., Saraiva, L. M., Pereira, I. A. (2003) A novel membrane-bound respiratory complex from Desulfovibrio desulfuricans ATCC 27774. *Biochim Biophys Acta*, vol. 1605, pp. 67–82

Rees C. E. (1973) Steady-state model for sulfur isotope fractionation in bacterial reduction processes. *Geochim. Cosmochim. Acta* 37, 1141–1162.

Robbins, P. W., Lipmann, F. (1958a) Enzymatic synthesis of adenosine-5'-phosphosulfate, *The Journal of Biological Chemistry*, vol. 233, pp. 686-690

Robbins, P. W., Lipmann, F. (1958b) Separation of the two enzymatic phases in active sulfate synthesis, *The Journal of Biological Chemistry*, vol. 233, pp. 681-685

Rudnicki M. D., Elderfield H., and Spiro B. (2001) Fractionation of sulfur isotopes during bacterial sulfate reduction in deep ocean sediments at elevated temperatures. *Geochim. Cosmochim. Acta* **65,** 777–789.

Sass H., Steuber J., Kroder M., Kroneck P. M. H., and Cypionka H. (1992) Formation of thionates by freshwater and marine strains of sulfate-reducing bacteria. *Arch. Microbiol.* **158,** 418–421

Shen, YA, Buick, R (2004) The antiquity of microbial sulfate reduction, *Earth Science Reviews*, 64, 243-272

Sørensen K. B. and Canfield D. E. (2004) Annual fluctuations in sulfur isotope fractionation in the water column of a euxinic marine Basin. *Geochim. Cosmochim. Acta* **68,** 503–515.

Strauss, H. (1993) Sulfur isotope record of Precambrian sulfate: new data and a critical evaluation of the existing record, *Precambrian Research*, v. 63, p. 225–246.

Strauss H (1997) The isotopic composition of sedimentary sulfur through time. *Palaeogeogr Palaeoclimatol Palaeoecol* 132(1):97–118.

Strauss, H., (1999) Geological evolution from isotope proxy signals—sulfur. *Chemical Geology* 161 (1–3), 89–101.

Sub Sim, M, Ono, S, Donovan, K, Templer, SP, Bosak, T (2011) Effect of electron donors on the fractionation of sulfur isotopes by a marine *Desulfovibrio* sp. *Geochimica et Cosmochimica Acta*, vol. 75, issue 15, pp. 4244-4259

Thode H. G. (1991) Sulphur isotopes in nature and the environment: An overview. In *Stable Isotopes in the Assessment of Natural and Anthropogenic Sulphur in the Environment* (ed. H. R. Krouse and V. A. Grinenko), pp. 1–26, John Wiley & Sons Ltd.

Vainshtein M. B., Matrosov A. G., Baskunov V. P., Zyakun A. M., and Ivanov M. V. (1980) Thiosulfate as an intermediate product of bacterial sulfate reduction. *Microbiology* **49,** 672–675.

Venceslau, S. S., Lino, R. R. R., Pereira, I. A. C. (2010) The Qrc membrane complex, related to the alternative complex III, is a menaquinone reductase involved in sulfate respiration, *The Journal of Biological Chemistry*, vol. 285, no. 30, pp. 22774-22783

Voordouw, G. (2002). Carbon monox- ide cycling by *Desulfovibrio vulgaris* Hildenborough. *J. Bacteriol.* 184, 5903–5911.

Walker, J.C.G., 1986. Global geochemical cycles of carbon, sulfur and oxygen. *Marine Geology* 70 (1–2), 159–174.

Werne J. P., Lyons T. W., Hollander D. J., Formolo M. J., and Damsté J. S. S. (2003) Reduced sulfur in euxinic sediments of the Cariaco Basin: sulfur isotope constraints on organic sulfur formation. *Chem. Geol.* **195,** 159–179.

Wood, P. M. (1978) Chemiosmotic model for sulfate respiration. *FEBS Lett*, vol. 95, pp. 12–18

Wortmann UG, Bernasconi SM, Bottcher ME (2001) Hypersulfidic deep biosphere indicates extreme sulfur isotope fractionation during single-step microbial sulfate reduction. *Geology* 29, 647–650.

Young E. D., Galy A. and Nagahara H. (2002) Kinetic and equilibrium mass-dependent isotope fractionation laws in nature and their geochemical and cosmochemical significance. *Geochim. Cosmochim. Acta* 66, 1095–1104.

Zane G, Yen H, Wall J (2010) Effect of the Deletion of qmoABC and the Promoter---Distal Gene Encoding a Hypothetical Protein on Sulfate Reduction in Desulfovibrio vulgaris Hildenborough. *Applied and Environmental Microbiology,* **76,** 5500-5509.